

## Gas flaring and resultant air pollution

Fawole, Olusegun G.; Cai, X. M.; Mackenzie, A. R.

DOI:

[10.1016/j.envpol.2016.05.075](https://doi.org/10.1016/j.envpol.2016.05.075)

License:

Creative Commons: Attribution-NonCommercial-NoDerivs (CC BY-NC-ND)

*Document Version*

Peer reviewed version

*Citation for published version (Harvard):*

Fawole, OG, Cai, XM & Mackenzie, AR 2016, 'Gas flaring and resultant air pollution: A review focusing on black carbon', *Environmental Pollution*, vol. 216, pp. 182-197. <https://doi.org/10.1016/j.envpol.2016.05.075>

[Link to publication on Research at Birmingham portal](#)

**Publisher Rights Statement:**

Eligibility for repository: Checked on 8/7/2016

**General rights**

Unless a licence is specified above, all rights (including copyright and moral rights) in this document are retained by the authors and/or the copyright holders. The express permission of the copyright holder must be obtained for any use of this material other than for purposes permitted by law.

- Users may freely distribute the URL that is used to identify this publication.
- Users may download and/or print one copy of the publication from the University of Birmingham research portal for the purpose of private study or non-commercial research.
- User may use extracts from the document in line with the concept of 'fair dealing' under the Copyright, Designs and Patents Act 1988 (?)
- Users may not further distribute the material nor use it for the purposes of commercial gain.

Where a licence is displayed above, please note the terms and conditions of the licence govern your use of this document.

When citing, please reference the published version.

**Take down policy**

While the University of Birmingham exercises care and attention in making items available there are rare occasions when an item has been uploaded in error or has been deemed to be commercially or otherwise sensitive.

If you believe that this is the case for this document, please contact [UBIRA@lists.bham.ac.uk](mailto:UBIRA@lists.bham.ac.uk) providing details and we will remove access to the work immediately and investigate.

1	<b>Table of Content</b>	
2	1 Introduction.....	5
3	1.1 Motivation.....	5
4	1.2 Review summary.....	7
5	1.3 Global oil and gas reserves.....	8
6	1.4 Temporal and geographical trends in gas flaring.....	9
7	2 Oil and Gas Production.....	15
8	2.1 Exploration and exploitation.....	15
9	2.2 Composition of natural gas.....	16
10	2.3 Thermodynamic properties of varying fuel gas compositions.....	18
11	3 Overview of the gas flaring processes.....	19
12	3.1 Gas flaring emission and its environmental impact.....	20
13	3.2 Emissions measurements around real-world gas flaring sites.....	23
14	3.3 Types of Flares.....	26
15	3.3.1 Steam- Assisted Flare.....	27
16	3.3.2 Air-Assisted Flare.....	28
17	3.3.3 Pressure-Assisted Flare.....	29
18	3.3.4 Non-Assisted Flare.....	29
19	4 Estimating emissions from gas flaring.....	31
20	4.1 Determining the flame regime.....	31
21	4.2 Emission factors (EF) for gas flaring emissions.....	33
22	4.3 Soot emission from gas flaring.....	35
23	4.4 Scaling soot emission from lab-based studies.....	38
24	4.5 Soot modelling.....	41
25	4.6 Gas flaring emissions in global models and inventories.....	43
26	5 Conclusion.....	44
27	6 Glossary.....	47
28	7 References.....	48
29		
30		
31		

## 32 **Gas flaring and resultant air pollution: A review focusing on Black Carbon**

33 Olusegun G. Fawole<sup>1,3</sup>, X. -M. Cai<sup>1</sup> and A. R. MacKenzie<sup>1, 2\*</sup>

34 <sup>1</sup>School of Geography, Earth and Environmental Sciences, University of Birmingham,  
35 Edgbaston, Birmingham, B15 2TT, UK

36 <sup>2</sup>Birmingham Institute of Forest Research, University of Birmingham, Edgbaston,  
37 Birmingham, B15 2TT, UK

38 <sup>3</sup>Environmental Research Laboratory, Department of Physics, Obafemi Awolowo University,  
39 Ile-Ife, Nigeria 220005

40 \*Corresponding author: a.r.mackenzie@bham.ac.uk

### 41 **Abstract**

42 Gas flaring is a prominent source of VOCs, CO, CO<sub>2</sub>, SO<sub>2</sub>, PAH, NO<sub>x</sub> and soot (black  
43 carbon), all of which are important pollutants which interact, directly and indirectly, in the  
44 Earth's climatic processes. Globally, over 130 billion cubic metres of gas are flared annually.  
45 We review the contribution of gas flaring to air pollution on local, regional and global scales,  
46 with special emphasis on black carbon (BC, "soot"). The temporal and spatial characteristics  
47 of gas flaring distinguishes it from mobile combustion sources (transport), while the open-  
48 flame nature of gas flaring distinguishes it from industrial point-sources; the high  
49 temperature, flame control, and spatial compactness distinguishes gas flaring from both  
50 biomass burning and domestic fuel-use. All of these distinguishing factors influence the  
51 quantity and characteristics of BC production from gas flaring, so that it is important to  
52 consider this source separately in emissions inventories and environmental field studies.  
53 Estimate of the yield of pollutants from gas flaring have, to date, paid little or no attention to  
54 the emission of BC with the assumption often being made that flaring produces a smokeless  
55 flame. In gas flares, soot yield is known to depend on a number of factors, and there is a need

56 to develop emission estimates and modelling frameworks that take these factors into  
57 consideration. Hence, emission inventories, especially of the soot yield from gas flaring  
58 should give adequate consideration to the variation of fuel gas composition, and to  
59 combustion characteristics, which are strong determinants of the nature and quantity of  
60 pollutants emitted. The buoyant nature of gas flaring plume, often at temperatures in the  
61 range of 2000 K, coupled with the height of the stack enables some of the pollutants to escape  
62 further into the free troposphere aiding their long-range transport, which is often not well-  
63 captured by model studies.

64

#### 65 **Capsule Abstract**

66 The review identified gaps in the estimation of emissions from the gas flaring process and  
67 argues for explicit recognition of gas flaring emissions in emission inventories and global  
68 models.

69

#### 70 **Keywords**

71 Gas flaring; Oil and gas; Black Carbon; Incomplete combustion; Hydrocarbon; Emission  
72 factors

73

74

75

76

77

78

79 ***Variables used and their meanings***

80  $u_e$  exit velocity of the flue gas ( $\text{m s}^{-1}$ )

81  $s$  the air-fuel ratio

82  $\rho_e, \rho_\infty$  the fuel gas and ambient densities respectively ( $\text{kg m}^{-3}$ )

83  $g$  acceleration due to gravity ( $\text{m s}^{-2}$ )

84  $\Delta T_f$  mean peak flame temperature rise, K (taken as the difference between the adiabatic  
85 flame temperature and the ambient temperature)

86  $d_e$  burner diameter (m)

87  $\nu_o$  kinematic viscosity of the gas-air mixture ( $\text{m}^2 \text{s}^{-1}$ )

88  $L$  characteristic flame length (m)

89  $\dot{m}_o$  mass flux of the flue gas at the burner exit ( $\text{kgm}^{-2}\text{s}^{-1}$ )

90  $f_s$  stoichiometric mixture fraction

91  $\phi$  equivalence ratio

92  $T_\infty$  ambient temperature

93

94

95

96

97

98

## 99 **1 Introduction**

### 100 **1.1 Motivation**

101 Humans need energy to drive their technology: and hence, make life pleasurable and worth  
102 living. Different forms of energy are in use and new ones are developed in order to meet the  
103 increasing needs of society (MacKay, 2008). This quest for dependable, affordable and  
104 environmentally benign energy sources has occurred throughout human history; for the last  
105 century or so, crude oil has been the focus of world energy. In 2011, crude oil was estimated  
106 to provide 52.8 % of the world's energy (13113 Mtoe); with oil and natural gas accounting  
107 for 31.5 % and 21.3 % respectively (IEA, 2013).

108 Human reliance on oil and gas as an energy source is not without its attendant impact on the  
109 environment. During production, detrimental impacts on the environment (air, water and soil)  
110 include: oil spills and leakages; venting; sludge disposal; and flaring (Almanza et al., 2012;  
111 Osuji and Adesiyan, 2005; Osuji and Onojake, 2004; Sonibare et al., 2010). The post-  
112 production impact of oil and gas on the environment is also a major source of concern, but is  
113 not the subject of this review.

114 Gas flaring is often a routine daily activity in oil fields around the world, particularly in oil-  
115 rich regions of the world where the infrastructure to capture, store and utilise the gas  
116 produced is not available. Flaring is most often associated with Nigeria and the Russian  
117 Arctic, but it does still occur in more developed economies: the North Dakota Bakken shale  
118 region, for instance (see, e.g., <http://www.eia.gov/todayinenergy/detail.cfm?id=23752>, last  
119 accessed on 29 January 2016). Despite several calls by international bodies such as the World  
120 Bank's Global Gas Flaring Reduction (GGFR) initiative, the volume of gas flared globally  
121 appears to have plateaued at around 130 billion cubic metres (bcm) since 2008, or may even  
122 have increased (see section 1.4, below). According to GGFR (2013), there was an increase of  
123 2 bcm in the volume of gas flared in 2011 compared to the previous year. The latest in this

124 series of initiatives by the World Bank - Zero Routine Flaring by 2030 - was launched by the  
125 Secretary-General of the United Nations, Ban Ki-Moon and World Bank's President, Jim  
126 Yong Kim, in May, 2015 (see [http://www.worldbank.org/en/programs/zero-routine-flaring-](http://www.worldbank.org/en/programs/zero-routine-flaring-by-2030)  
127 [by-2030](http://www.worldbank.org/en/programs/zero-routine-flaring-by-2030), last accessed on January 29, 2016).

128 Gas flaring, a prominent source of black carbon (BC) and other pollutants, has been ignored  
129 or underestimated in emission inventories and models, as a result of which models are  
130 struggling to predict measurements of BC in regions of intense gas flaring. The intensity of  
131 gas flaring and specifics of atmospheric transport can combine to enhance the role of gas  
132 flaring emissions over very large areas (e.g., the Arctic) (Stohl et al., 2013). Presently,  
133 treatment of emissions from gas flaring is rather rudimentary in most global emission  
134 inventories. As at 2015, to the best of our knowledge, only two global pollutants inventories  
135 explicitly accounted for emissions from gas flaring (see section 4.5).

136 Gas flaring is classified as a miscellaneous BC-rich source, a group which includes aviation  
137 and shipping which together contribute about 9 % to global BC emission (Bond et al., 2013).  
138 Gas flaring is a very different type of combustion compared to other BC sources in this  
139 category; gas flaring is characterised by either fuel-regulated or oxidant-regulated open-fire  
140 (see below) resulting in flames that can be 8-10 metres in length, with flame temperature as  
141 high as 2000K. Gas flaring is a year-round activity in most of the intensive flaring regions of  
142 the world, and so differs from transport sources in being stationary and differs from other  
143 stationary sources (e.g. cooking and biomass burning) by being relatively constant in time.  
144 The GAINS (Greenhouse gas Air pollution INteractions and Synergies) model estimated that  
145 gas flaring contributes about 4 % of total anthropogenic BC emissions, majority of which are  
146 from the leading gas-flaring nations; Russia, Nigeria, and countries in the Middle East (Bond  
147 et al., 2013; Stohl et al., 2013). Gas flaring is estimated to contribute 260 Gg to global BC  
148 estimates annually (Bond et al., 2013), while in Russia, it is estimated to have the largest

149 contribution of 36.2 % to anthropogenic BC emission (Huang et al., 2015). From a 3-year  
150 model simulation, more than 40% of annual mean BC near the surface in the Arctic is  
151 estimated to be contribution from gas flaring (Stohl et al., 2013).

152 Considering the small number of nations that still flare gas, a contribution of 4 % to global  
153 BC represents a significant skew in the global apportionment of BC emissions. On a regional  
154 scale, the contribution of this ‘overlooked’ source of ambient aerosol loading is likely to be  
155 significant.

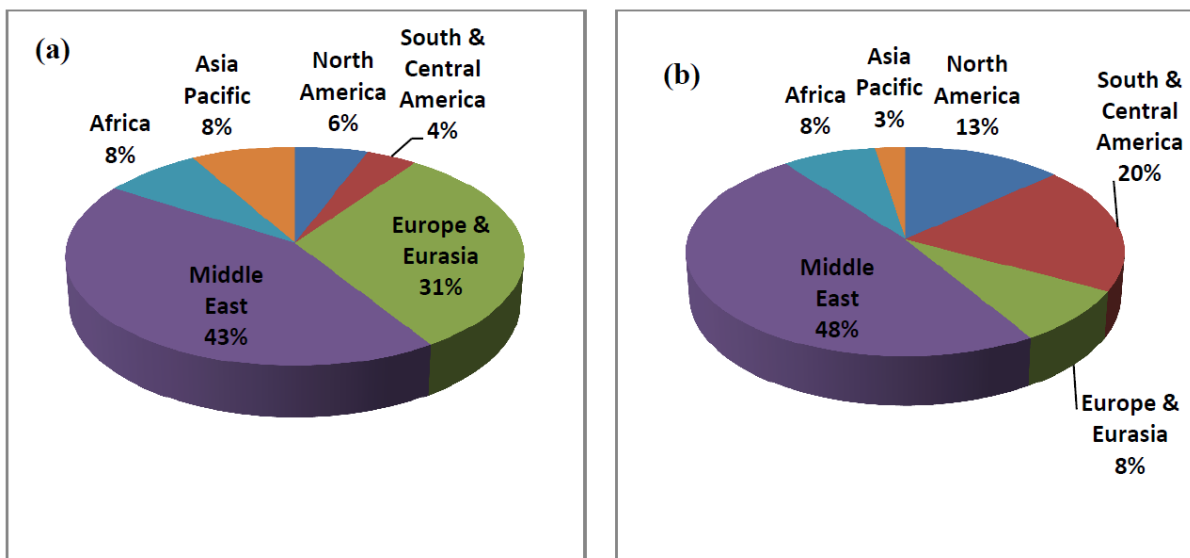
## 156 **1.2 Review summary**

157 For this review, we have collated previous studies (1984-2015) on gas flaring and its  
158 contributions to ambient aerosol loadings. This review is the first to cover virtually every  
159 aspects of gas flaring (process, trends, chemistry, flame dynamics and environmental impact).  
160 The review starts with a brief assessment of the level and distribution of oil and gas reserves  
161 around continents of the world. Compositional variation of the natural gas flared and their  
162 thermodynamic properties are discussed because they are likely to have significant impact on  
163 pollutant emission rates and overall amount. Next, we provide a discussion of the temporal  
164 and geographical trends in gas flaring, including brief comments about how weather  
165 conditions in regions where gas flaring is common will impact near-field dispersion and long-  
166 range transport. This is followed by a broad discussion of the gas flaring process itself;  
167 highlighting how engineering and technology decisions impact on the emission of air  
168 pollutants. Finally, several techniques used to estimate emissions from gas flaring are  
169 discussed. Throughout this review, special attention is paid to soot (i.e. carbonaceous aerosol  
170 predominantly composed of BC) emission from gas flaring because of the now known  
171 contribution of BC to global warming and the apparent neglect of the contribution of gas  
172 flaring to ambient air aerosol loadings in inventories and global models.



173 **1.3 Global oil and gas reserves**

174 World-proven natural gas and oil reserves at the end of 2012 stood at 187.3 and 1668.9  
175 trillion cubic metres (tcm) respectively, sufficient to meet 55.7 years of global production  
176 (BP, 2013). The distribution of these reserves among regions of the world is shown in Figures  
177 1(a) and (b). The natural gas collected during the exploration of crude oil from the Earth's  
178 crust can be a very good source of fuel; transported in pipes for industrial or domestic use and  
179 also recycled back into the processing operation (Davoudi et al., 2013; Elvidge et al., 2009).  
180



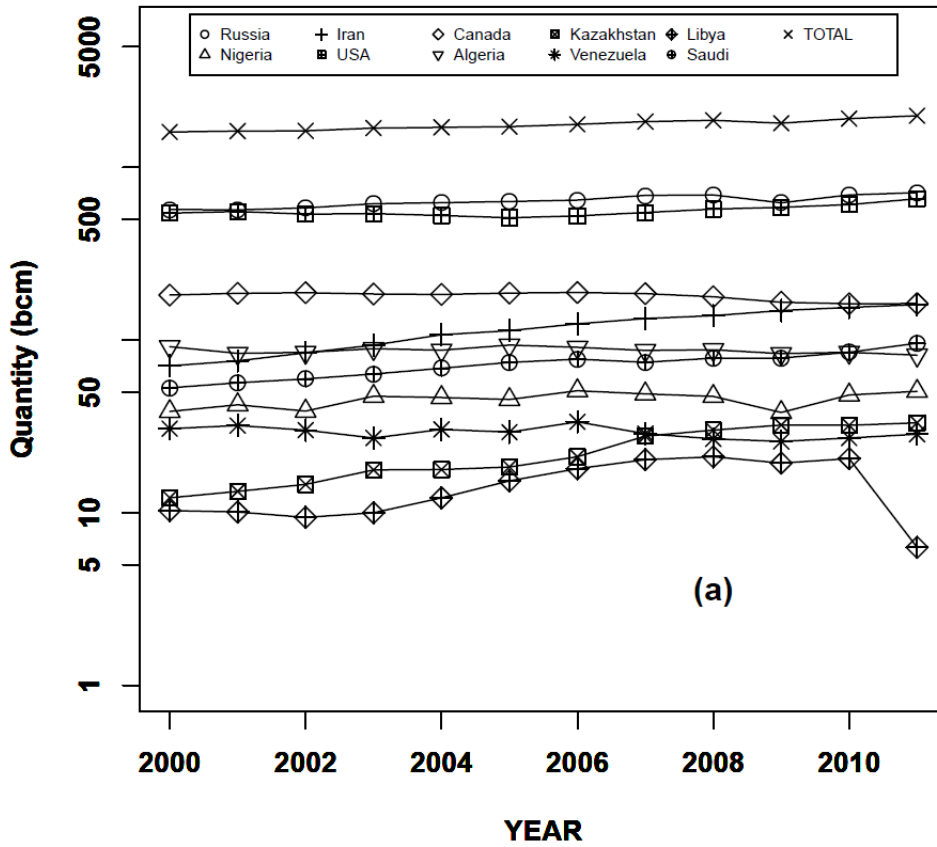
181 **Figure 1:** (a) The distribution of world natural gas reserves (b): The distribution of world oil  
182 reserves (adapted from BP (2013)).  
183  
184

185 In developing countries and oil-rich regions where the technology, infrastructure, and market  
186 structure to put all of the natural gas to meaningful use are not available or inadequate, the  
187 excess natural gas then becomes a waste stream and is flared or vented. Gas flaring has been  
188 termed ‘gross waste’ by the World Bank’s initiative against gas flaring (Global gas flaring  
189 reduction: GGFR), because flaring represents direct injection of fossil carbon into the  
190 atmosphere without capture and utilization of the heat produced by combustion.

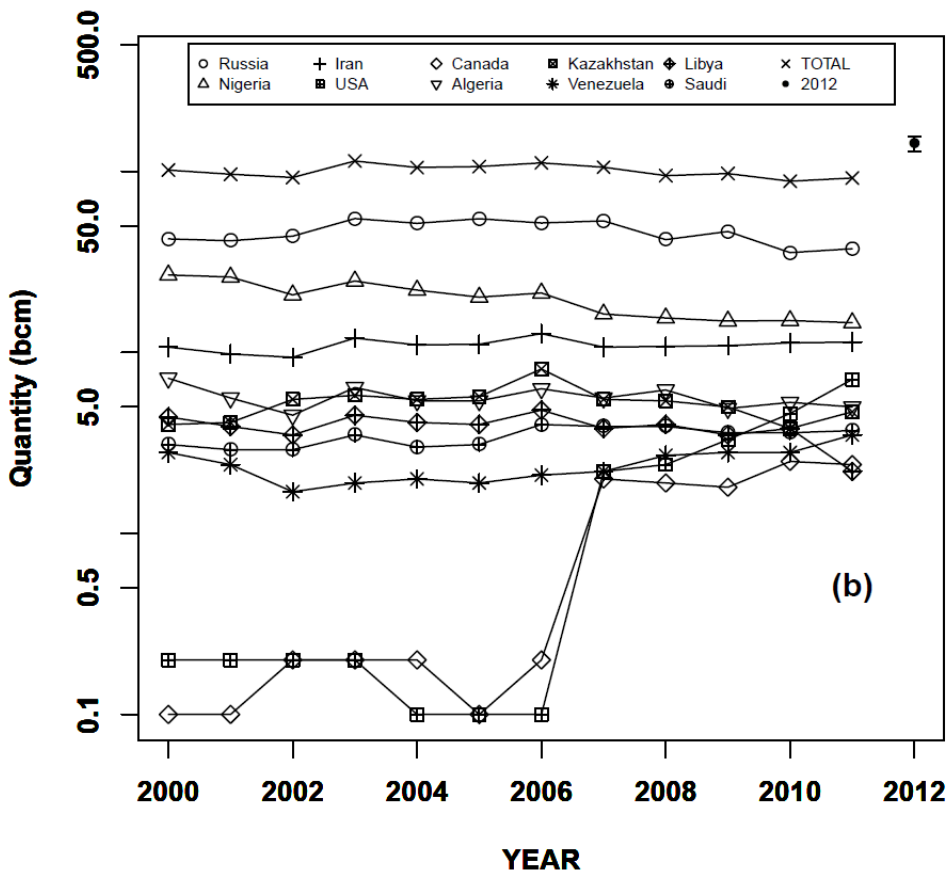
191 **1.4 Temporal and geographical trends in gas flaring**

192 The all-time peak of volume of gas flared, 172 bcm, was in 2005 (Elvidge et al., 2009).  
193 Figure 2(a) shows the quantity of natural gas produced by the top 10 oil producing nations of  
194 the world between 2000 and 2011, and for comparison, Figure 2(b) shows the estimated  
195 quantity of gas flared by these major oil producing nations during the same period of time.  
196 The estimated volume of gas flared globally in 2012 is also shown in Figure 2(b): the 2012  
197 data is obtained from Elvidge et al. (2015). Data for the plots in figure 2(a) and (b) are from  
198 IEA (2012) and GGFR (2012), respectively. Between 2008 and 2011, there was no  
199 significant decrease in the amount of natural gas flared. In fact, there was a slight increase  
200 between 2010 and 2011. According to (BP, 2015), the production excludes the quantity flared  
201 or recycled. Therefore, total fossil fuel extracted and ultimately released to the environment is  
202 the sum of the production and quantity flared.

203 Figure 3 gives the temporal variation of the fraction of total gas extracted that is flared  
204 between 2000 and 2011. Nigeria, Libya and Kazakhstan still flare a sizeable amount of their  
205 total production. As at 2011, Nigeria and Libya flared about 30 % of their total gas extracted  
206 while Kazakhstan flares about 15 %. The 30 % (15.2 bcm) flared by Nigeria is more than  
207 twice Libya's total gas extracted (6.3 bcm) for the same period. Russia and Nigeria together  
208 account for about 35 % of the gas flared globally (Elvidge et al., 2009). Although the fraction  
209 of gas flared is decreasing for most countries and for the largest emitters, several countries  
210 show flat or increasing fractions of gas flared. The estimated quantity of natural gas flared in  
211 the US and Canada, as shown in Figure 2b, are just for the off-shore flaring which is  
212 presumably responsible for the very low quantities recorded. After 2006, there is a factor of  
213 22 and 10 increase in flaring from USA and Canada, respectively, resulting, presumably,  
214 from increased exploitation of unconventional hydrocarbon reservoirs ('fracking').

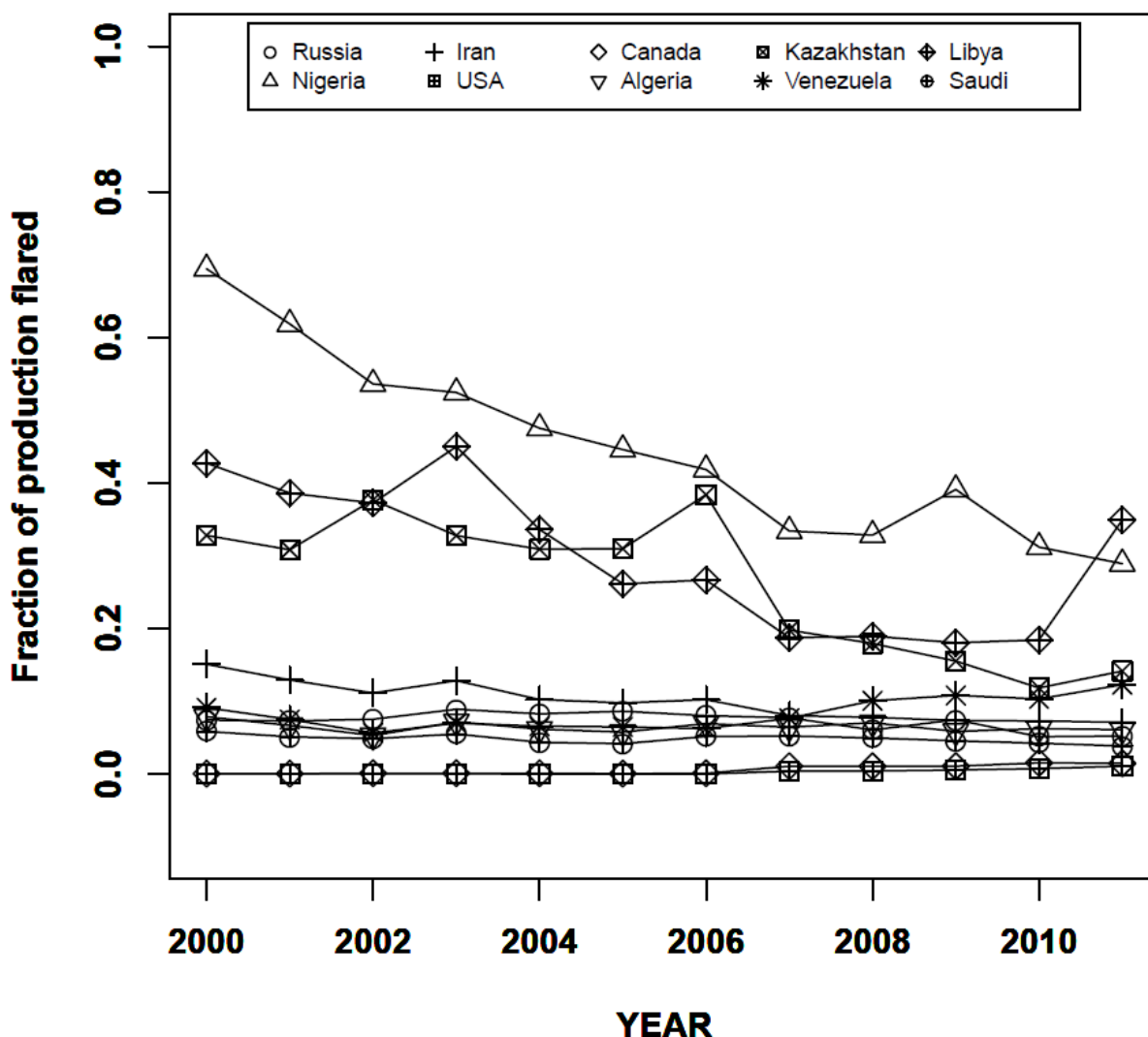


215  
216



217  
218  
219

**Figure 2:** Trend of natural gas (a) production and (b) flaring in major oil producing nations between 2000 and 2011 (adapted from IEA (2012) and (GGFR, 2012) respectively).



221 **Figure 3:** Trend of quantity flared compared to total production (data from Figure 2)

222  
 223  
 224  
 225 Table 1 gives the estimates, from satellite data, of the quantity of gas flaring by the top 20 gas  
 226 flaring nations of the world in 2008 and a brief summary of the climatic conditions of the  
 227 region based on the Köppen climate classification (see, e.g., Holden (2005))

228 Figure 4, reproduced, with permission, from Casadio et al. (2012), shows the global  
 229 geographic distribution of gas flaring sites obtained by remote sensing techniques. In Africa,  
 230 the flaring spots are clustered around the North - Algeria, Libya and Egypt - as well as around  
 231 the Atlantic Ocean especially the Niger Delta area of Nigeria. In Europe, they are around  
 232 Russia and Kazakhstan, and Iran, Iraq, Kuwait, and Saudi Arabia in the Middle East. Satellite

233 remote sensing not only gives a general picture of the spatial distribution of flares, but also a  
 234 gross estimation globally at national levels.

235 **Table 1:** Year 2008 estimated gas flared by top 20 gas flaring nations with an estimated error  
 236 of  $\pm 2.11$  bcm.

Rank	Country	Gas Flared (bcm)	Regional Climate	Comments*
1	Russia	40.5	(Dfa, Dfb, Dwa, Dwb), (Dfc, Dfd, Dwc, Dwd) and ET	peri-Arctic emissions; pole-ward atmospheric flow around Tibetan anticyclone in northern hemisphere winter
2	Nigeria	15.1	Am and Aw	Tropical monsoon and trade-wind littoral and tropical wet and dry climate resulting from West African monsoon winds that changes direction with season; climatic condition is controlled by trade wind and movement of the ITCZ
3	Iran	10.4	Bwh	Tropical and subtropical desert climate characterised by large diurnal temperature range. Deep turbulent boundary layer during the day; shallow stable boundary layer at night. Large-scale subsidence (descending branch of the Hadley circulation) above the boundary layer.
4	Iraq	7.0	Bsh	Mid-latitude steppe and desert climate characterised by semiarid annual rainfall distribution
5	Algeria	5.5	Bwh	As for Iran
6	Kazakhstan	5.2	Bwk	Mid-latitude arid wet and dry climate
7	Libya	3.8	Bwh	As for Iran
8	Saudi Arabia	3.5	Bwh	As for Iran
9	Angola	3.1	Cwa	Humid subtropical climate; equatorward and poleward circulation during winter and summer respectively cause changes in the movement of air masses from the cold polar and warm tropics within this climate.
10	Qatar	3.0	Bwh	As for Iran
11	Uzbekistan	2.7	Csa	Mediterranean climate; it is controlled by the variation between subtropical high in summer and

12	Mexico	2.6	Af, Aw, Bsh, Bsk, Bwh, Cwa, Cwb, Cfa, Cfb	polar westerlies in winter Complex climatic condition; two tropical, two dry and three temperate climates
13	Venezuela	2.6	Aw	Tropical wet-dry climate
14	Indonesia	2.3	Aw, Am	As for Nigeria (see comment above)
15	USA	2.3	Bsk, Bsh, Bwk, Csa, Csb, Af	Mediterranean/dry summer subtropical climate characterised by moist winter and hot dry summer; subtropical anticyclones are key factor that control this climate
16	China	2.3	Cfa, Cwa	Humid subtropical climate; during winter the climate is influenced by the Siberian cold and during summer there is an inflow warm of air from the west
17	Oman	1.9	Bwh	As for Iran
18	Malaysia	1.9	Af	Tropical rainforest characterised by constant high temperatures and evenly distributed high precipitation; controlled by movement of the ITCZ and rising air along trade wind coast. Strongly affected by el Nino Southern Oscillation
19	Canada	1.8	Dfb, Dfd, Dsc, Af	As for Russia (see above)
20	Kuwait	1.8	Bwh	As for Iran
	<b>TOTAL</b>	<b>119.3</b>		

237 **Source:** Quantity of gas flared is obtained from Elvidge et al. (2009). \*See Holden (2005)

238

239

240 Elvidge et al. (2015), using data collected by National Aeronautics and Space

241 Administration/National Oceanic and Atmospheric Administration Visible Infrared Imaging

242 Radiometer Suite (VIIRS), identified more than 7000 active flare globally in 2012: the bulk

243 of which were found in the upstream sector of the oil and gas industries. In 2012, the

244 estimated volume of gas flared globally is  $143 \pm 13.6$  bcm (Elvidge et al., 2015). Compared to

245  $119.3 \pm 2.11$  bcm estimated for 2008 (Elvidge et al., 2009), this is an increment of about 20 %

246 in the central tendencies of the estimates for both years and is well outside the combined

247 uncertainty bounds of both estimates. An increment of about 20 % over four years, stands in

248 stark contrast to the decrease anticipated as a result of the World Bank's Global Gas Flaring

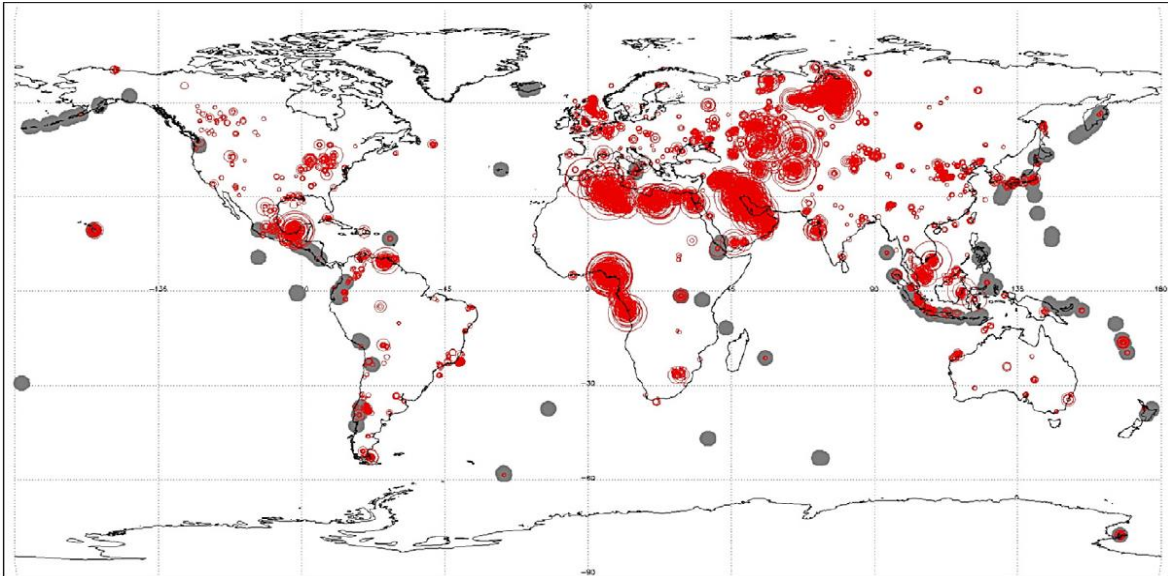
249 Reduction (GGFR) initiative. A new dimension to the problem is the inclusion of three new  
250 countries – India, Egypt and Turkmenistan - in the list of top 20 gas flaring countries.

251 The geographical location of the sources of gas flaring emissions (as monitored from space,  
252 see Figure 4), the atmospheric behaviour of emitted pollutants, and the pollutant “matrix”  
253 from other sources into which emission are made, determine to a large extent the effect gas  
254 flaring emissions will have on regional pollution loadings and on climate. BC emissions in  
255 the peri-Arctic and West African Monsoon (WAM) regions have the potential to interact with  
256 regional radiative energy budgets and atmospheric circulations, leading to impacts on their  
257 respective regional climates. Gas flaring emissions in the tropics, especially the WAM and  
258 South Asian Monsoon (SAM), could have significant regional impact as a result of the  
259 intense convective activities and cloud formation in these regions.

260 Monsoon circulations are characterised by large-scale seasonal reversals of wind regimes.  
261 Regions often referred to as ‘monsoonal’ include tropical and near-tropical regions which  
262 experience a summer rainfall maximum and most of these regions have a double rainfall  
263 maximum (Barry and Chorley, 2009). The annual climatic regime over West Africa has many  
264 similarities to that of South Asia. Both are characterised by surface air-flow which is  
265 determined by the position of the leading edge of a monsoon trough. Winds are south-  
266 westerly to the south of the trough and north-easterly to the North. The lack of a large  
267 mountain range in the north of West Africa strongly enhances the northward advance of the  
268 WAM compared to its South Asian counterpart. The position of the leading edge of the  
269 WAM trough may oscillate greatly from day-to-day through several degrees of latitude  
270 (Barry and Chorley, 2009). In the WAM, deep convection occurs in organised systems  
271 known as Mesoscale Convective Systems (MCS) (Mari et al., 2011; Mathon and Laurent,  
272 2001). Deep convection in the tropics associated with the ITCZ is responsible for intense

273 mixing, venting of the atmospheric boundary layer, and long-range transport of aerosol (Law  
274 et al., 2010; Reeves et al., 2010; Sultan and Janicot, 2003).

275



276 **Figure 4:** Flaring hot spot sites (1991-2009) as monitored from space are indicated as red  
277 spots while grey spots represent position of active volcanoes during the same period Casadio  
278 et al. (2012).  
279

## 280 **2 Oil and Gas Production**

### 281 **2.1 Exploration and exploitation**

282 Oil exploration can be a very complex and capital intensive process as oil deposits are often  
283 located in reservoirs buried far into the Earth. These locations can be in very remote and  
284 inhospitable parts of the Earth and can be either on- or off-shore. The multi-staged process of  
285 exploration, exploitation and processing of crude oil in its raw form from the Earth's crust  
286 can be broadly divided into upstream, midstream and downstream. Environmental  
287 contaminants are expelled into the ambient environment - soil, air and water - at different  
288 stages of the process. Crude oil is found in reservoirs which also contain gas. This gas is  
289 known as "*associated natural gas*", and it is separated from the crude oil at a Flow Station.  
290 Natural gas includes both "*non-associated*" gas originating from fields producing only  
291 gaseous hydrocarbons, and "*associated*" gas produced in association with crude oil (IEA,



292 2012). Natural gas comprises mainly hydrocarbons, predominantly short-chained alkanes. At  
293 the separation stage, some of the natural gas is captured for domestic and industrial use while  
294 the rest is disposed of, usually by *flaring* in open flames. Below, we will use the term ‘fuel  
295 gas’ to refer to natural gas that is flared. The quantity of contaminants expelled at this stage  
296 of processing depends on the technology employed, quantity of crude oil processed, flare  
297 geometry and design, prevailing meteorological conditions and the composition of the flared  
298 gas (E & P Forum, 1994; Ismail and Umukoro, 2014; Johnson and Coderre, 2011; Obanijesu  
299 et al., 2009; Ouf et al., 2008; Sonibare and Akeredolu, 2004; Talebi et al., 2014).

300 Oil and gas are produced in many wells in different parts of the world at rates varying from  
301 50 m<sup>3</sup> to 700 m<sup>3</sup> per day. As a result of the diverse nature of the geological features of the  
302 area where these explorations take place, the composition of oil and gas varies from one  
303 station to another.

## 304 **2.2 Composition of natural gas**

305 The composition of natural gas from 10 stations from around the world is given in Table 2.  
306 Fuel gas is a combination of C<sub>1</sub> to C<sub>7+</sub> hydrocarbons which are predominantly alkanes. A  
307 typical fuel gas sample contains CH<sub>4</sub>, C<sub>2</sub>H<sub>6</sub>, C<sub>3</sub>H<sub>8</sub>, n-C<sub>4</sub>H<sub>10</sub>, i-C<sub>4</sub>H<sub>10</sub>, n-C<sub>5</sub>H<sub>12</sub>, i-C<sub>5</sub>H<sub>12</sub>, C<sub>6</sub>H<sub>14</sub>,  
308 C<sub>7</sub>H<sub>16</sub>, H<sub>2</sub>S, CO<sub>2</sub> and N<sub>2</sub>, where ‘n’ and ‘i’ stand for ‘normal’ i.e., straight chained, ‘iso’ or  
309 branched-chained alkanes, respectively. The separation of gas and liquid is not perfect at the  
310 Flow Stations and as such trace amounts of liquid can occur in the gas stream, enhancing the  
311 abundance of higher molecular weight alkanes in the fuel gas.

312 **Table 2:** Composition (in mole %) and Some Properties of Fuel Gas from Field Stations and Literature.

Composition	Flow Stations										Lab-based	
	1	2	3	4	5	6	7	8	9	10	A	B
<b>CH<sub>4</sub></b>	74.3	79.85	56.9	55.5	82.23	78.41	68.14	68.42	72.32	69.58	85.24	74.54
<b>C<sub>2</sub>H<sub>6</sub></b>	14.0	11.54	21.2	18.0	2.38	5.68	14.22	7.65	2.41	0.25	7.06	12.17
<b>C<sub>3</sub>H<sub>8</sub></b>	5.8	2.25	6.0	9.8	4.24	0.23	10.27	11.27	6.24	12.54	3.11	5.37
<b>nC<sub>4</sub>H<sub>10</sub></b>	2.0	2.58	3.7	4.5	0.94	0.70	3.23	4.39	8.12	2.35	1.44	2.49
<b>iC<sub>4</sub>H<sub>10</sub></b>	-	0.14	-	-	5.12	4.12	2.38	4.42	5.12	5.12	-	-
<b>nC<sub>5</sub>H<sub>12</sub></b>	0.9	3.24	1.6	1.6	2.25	9.12	0.75	0.94	3.14	5.20	-	-
<b>iC<sub>5</sub>H<sub>12</sub></b>	-	-	-	-	2.14	0.25	1.01	1.55	2.48	2.54	-	-
<b>C<sub>6</sub>H<sub>14</sub></b>	-	0.14	-	-	0.25	0.23	-	0.18	0.15	1.97	-	-
<b>N<sub>2</sub></b>	2.9	0.1	-	0.2	-	0.05	-	0.16	-	0.24	1.24	2.15
<b>CO<sub>2</sub></b>	-	0.16	7.1	8.9	0.45	1.21	-	1.02	-	0.21	1.91	3.28
<b>H<sub>2</sub>S</b>	0.1	-	3.5	1.5	-	-	-	-	0.02	-	-	-
<b>*C:H</b>	0.2659	0.2715	0.2569	0.2602	0.2730	0.2751	0.2860	0.2852	0.2893	0.2924	0.2541	0.2570
<b>*Molar mass (g mol<sup>-1</sup>)</b>	21.4	21.4	25.8	26.9	22.9	24.7	24.3	25.8	27.0	28.6	19.2	21.5
<b>*Molar mass (g mol<sup>-1</sup>) without CO<sub>2</sub> and N<sub>2</sub></b>	20.5	21.3	22.7	22.9	22.7	24.1	24.3	25.3	27.0	28.4	18.0	19.4
<b>*HHV (MJ m<sup>-3</sup>)</b>	44.8	46.4	47.8	48.7	49.1	52.0	52.2	54.2	57.2	60.3	39.8	42.5

313 2 and 5 – 10 are adapted from Sonibare and Akeredolu (2004), 1, 3 and 4 from Ismail and Umukoro (2014) and lab-based (A&B) from McEwen and Johnson (2012)

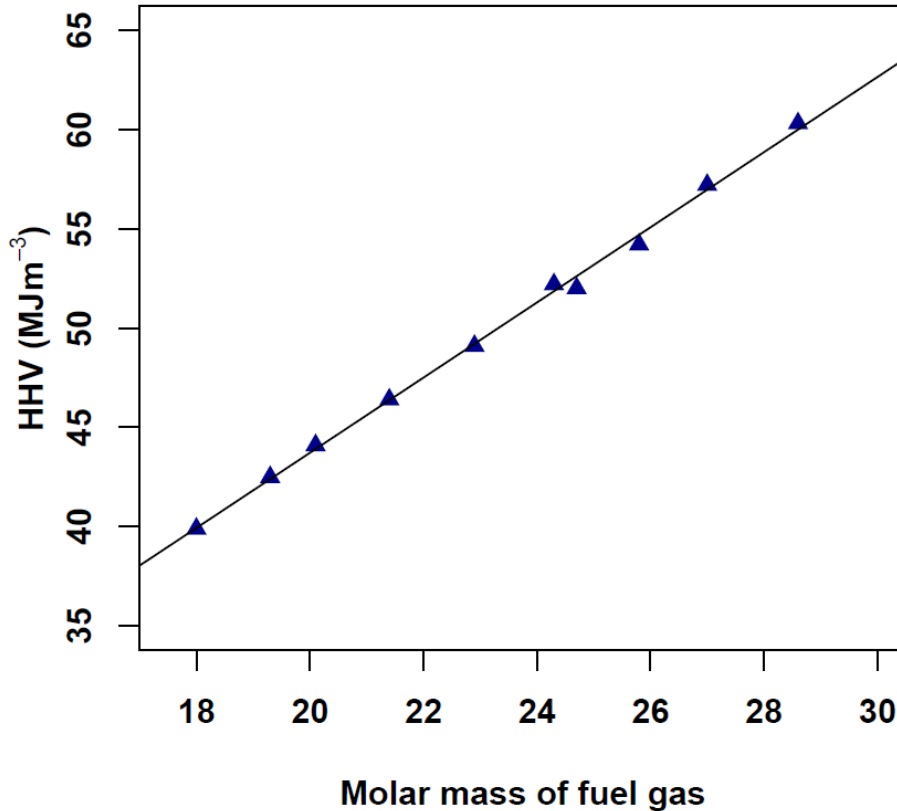
314 Compositions 1, 3 and 4 are from Saudi Arabia, Kuwait and Iraq respectively while 2 and 5 - 10 are from different flow stations in Nigeria.

315 C:H = mass-weighted carbon to hydrogen ratio

316 \* evaluated in this work

317 **2.3 Thermodynamic properties of varying fuel gas compositions**

318 The higher heating value (HHV) is the total enthalpy of the complete combustion reaction for  
319 the gas mixture, plus the heat of condensation of the water produced during combustion;  
320 lower heating value (LHV) is the total enthalpy of the complete combustion when water  
321 remains present in its gaseous form only (Flagan and Seinfeld, 2012). The Volumetric  
322 heating value (VHV), measured in  $\text{kJ mol}^{-1}$ , usually refer to the HHV unless otherwise stated.  
323 In gas flaring, HHV, calculable using data from standard thermodynamic tables, defines the  
324 total amount of energy available to provide buoyancy to the flare. Buoyancy is an important  
325 parameter in determining the dispersion of flare emissions (Beychok, 1994; Leahey and  
326 Davies, 1984). The heat content of a fuel gas depends on its molar mass and by extension the  
327 density of the fuel. Figure 5 presents the best fit line relating HHV to the molar mass of the  
328 fuel gases from the Flow Stations given in Table 2. This plot shows the extent of dependence  
329 of HHV on the molar mass, and hence, density of the fuel gas. These properties of the fuel  
330 gas, varies with the fuel composition. Note that the HHV values for the laboratory flares in  
331 Table 1 are lower than the HHV for the Flow Station fuel gases.



332  
 333 **Figure 5:** Higher heating value (HHV) as a function of molar mass of fuel gas for the Flow  
 334 Station data reported in Table 1.

### 335 **3 Overview of the gas flaring processes**

336 Gas flaring is carried out with the aim to convert its hydrocarbon content, especially methane,  
 337 to products that are less hazardous to the immediate vicinity of the flare site. Gas flaring is  
 338 classified as a stationary combustion source for the purpose of air pollution regulation  
 339 (USEPA, 2008). The combustion process involves the rapid oxidation of the fuel gas with the  
 340 release of heat, gaseous and particulate pollutants, whose nature and quantity depend on the  
 341 amount and composition of gas fuel burned, the combustion characteristics as well as the  
 342 flare geometry and design (Ouf et al., 2008; Torres et al., 2012a).

343 Gas flaring may be categorized as *emergency*, *process* and *production* flaring depending on  
 344 the basis of the flaring (Johnson and Coderre, 2011). *Emergency flaring* is unplanned: it is  
 345 carried out at large facilities for safety purposes for a short duration of time. During

346 emergency flaring, a large volume of gas is disposed of quickly and, hence, the flow rate of  
347 the fuel gas is very high. *Process flaring* is an intermittent disposal of unwanted gas that may  
348 last for a few hours or a couple of days at often low flow rate. It occurs during well-testing as  
349 well as start-up and shutdown of process units. *Production flaring* may occur continuously  
350 for years as long as the oil is being explored and exploited. The flow rate can be very high at  
351 particular times especially during the initial development of a gas well (Johnson and Coderre,  
352 2011). As a result of the length of time involved, which can be years, and the flow rate of the  
353 gas flared, production flaring is the major process of concern for regional and global  
354 pollution, including interaction with climate.

### 355 **3.1 Gas flaring emission and its environmental impact**

356 Gas flaring is the process of disposing of gas (referred to as fuel gas in this review), by  
357 combustion in an open flame in the open atmosphere, using a burner tip designed specifically  
358 for that purpose, in the course of routine oil and gas production operations (McEwen and  
359 Johnson, 2012; OGP, 2000; Stone et al., 1992). Gas flaring is a source of greenhouse gases,  
360 precursor gases, VOCs, polycyclic aromatic hydrocarbon (PAH) and particulate matter (PM)  
361 in the form of soot (Ana et al., 2012; Johnson et al., 2013; McEwen and Johnson, 2012;  
362 USEPA, 2011; USEPA, 2012). These pollutants have been identified to have serious  
363 detrimental impact on animals, vegetation and human (Burney and Ramanathan, 2014; Dung  
364 et al., 2008; Pope III et al., 2002; USEPA, 2010). The *soot* emitted from the combustion of  
365 natural gas is predominantly *black carbon (BC)* (Johnson et al., 2013; Smith and Chughtai,  
366 1995).

367 BC is a strong climate forcer and plays a prominent role in the nature of the Earth's climate  
368 because of its ability to absorb solar radiation, and hence, to result in a changed vertical  
369 gradient of warming by incoming solar radiation (Ramana et al., 2010; Ramanathan and  
370 Carmichael, 2008). It also affects cloud processes as well as decreasing surface albedo on ice

371 and snow causing them to melt faster (IPCC, 2007). It can be short-lived in the atmosphere,  
372 as it is removed from the atmosphere by dry and wet deposition (although insoluble in water,  
373 it is wettable, particularly when ‘aged’ by atmospheric oxidation). When mixed with other  
374 aerosol components in the atmosphere, BC can affect the climate for longer as its residence  
375 time is increased in that state (Bond et al., 2013; Flanner et al., 2007; Quinn et al., 2008;  
376 Ramana et al., 2010). Within current estimated uncertainties, BC is the second highest  
377 contributor to global warming just after CO<sub>2</sub> (IPCC, 2007), and also the main light-absorbing  
378 component of atmospheric aerosols (Bond et al., 2013; Chung and Seinfeld, 2005; Jacobson,  
379 2002; Ramanathan and Carmichael, 2008; Seinfeld, 2008).

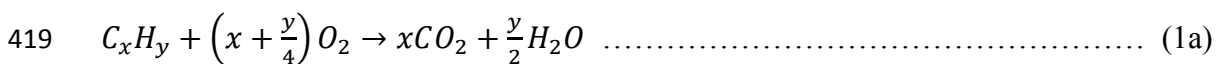
380 The radiative forcing capacity of a cloud of aerosol particles depends on the ratio of the BC  
381 to other components in the cloud (Ramana et al., 2010). The ubiquitous nature of BC coupled  
382 with its several effects on the Earth’s climate makes the study of its sources and emission  
383 rates important. If adequate measures are put in place to reduce BC emission, short-term  
384 reduction of radiative forcing can be achieved in the Arctic and other oil rich regions of the  
385 world (Arctic Council, 2013; Feichter and Stier, 2012; Tripathi et al., 2005).

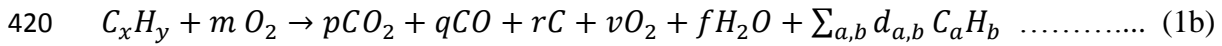
386 Studies have shown that the contributions from oil and gas processing, especially gas flares,  
387 to air pollution have been severely underestimated (Edwards et al., 2013; Johansson et al.,  
388 2014; Schultz, 2014; Stohl et al., 2013). This is arguably due to the fact that emission factors  
389 (EF) often used to estimate the emissions of pollutants from the oil and gas sector, especially  
390 gas flaring, are too general and independent of site specifics such as fuel composition and  
391 combustion characteristics. There is a pressing research need for more measurements and  
392 development of EFs estimates that vary with the fuel gas composition and combustion  
393 characteristics.

394 At the local scale, ground-level measurements within one kilometre downwind of the flaring  
395 sites have indicated an elevated concentration of particulate and gaseous pollutants (Edwards

396 et al., 2013; Obanijesu et al., 2009; Sonibare et al., 2010). Likewise, on a regional scale,  
 397 flight campaign during ACCESS (Arctic Climate Change Economy and Society) around oil  
 398 and gas installations in Heidrun, Norway reported elevated concentrations of NO, SO<sub>2</sub> and  
 399 CO in the lower troposphere (Roiger et al., 2015).

400 NO<sub>x</sub> (NO+NO<sub>2</sub>), SO<sub>2</sub>, CO<sub>2</sub>, CO and unburned hydrocarbon are the major pollutant  
 401 constituents of gas flaring plumes (USEPA, 1995). The low amount of the nitrogen and  
 402 sulphur content of the fuel gas notwithstanding, the NO<sub>x</sub> and SO<sub>2</sub> emission from gas flaring  
 403 remain significant because the ambient background level of both pollutants are usually low.  
 404 Hence, gas flaring can substantially enhance the local concentrations of these pollutants.  
 405 Complete combustion is often not achieved in most flaring conditions (Leahey et al., 2001).  
 406 During incomplete combustion, methane (CH<sub>4</sub>) and other unburned components of the fuel  
 407 gas are given off and some fuel components are partially oxidized to CO and soot rather than  
 408 completely oxidised to CO<sub>2</sub> (RTI, 2011; Strosher, 2000; Villasenor et al., 2003). Equations 1a  
 409 and b, respectively, give simplified equations for the 'ideal' complete and partial oxidation of  
 410 the fuel gas. In equation (1b), 'rC' denotes soot production, 'vO<sub>2</sub>' excess oxygen in the case of  
 411 fuel-lean combustion and 'C<sub>a</sub>H<sub>b</sub>' are PAH and other semi-volatile organics resulting from the  
 412 pyrolysis of hydrocarbons in the fuel gas. The value of *m* in equation (1b) determines a fuel-  
 413 lean (over-fired;  $m > x + y/4$ ) or fuel-rich (under-fired;  $m < x + y/4$ ) combustion process. The  
 414 level of combustion (oxidation) of the fuel gas is dependent on a number of factors: the  
 415 nature of the flame during combustion, the level of mixing of the gas and air in the reaction  
 416 zone, the amount of oxidant (oxygen) available, the VHV of the fuel gas and the prevailing  
 417 condition of the ambient wind (Stone et al., 1992). Flare design and geometry are also key  
 418 determinants of the level of combustion of the fuel gas.





421 For ‘ideal’ complete combustion, the oxidation of the hydrocarbon yields carbon dioxide and  
422 water only (equation 1a), while the oxidation of the sulphur (as H<sub>2</sub>S) and nitrogen content of  
423 the fuel gas gives SO<sub>2</sub> and NO<sub>x</sub> respectively. In gas flaring, NO<sub>x</sub> is produced by thermal  
424 cracking of the nitrogen content of the fuel gas and entrained atmospheric nitrogen. The  
425 amount of carbon-containing emission (CO<sub>2</sub>, CO, C<sub>a</sub>H<sub>b</sub>, and BC) given off depends on the  
426 molar mass of non-CO<sub>2</sub> carbon per mole of the fuel gas (cf. Table 2). Smoking of a gas flare  
427 does not necessarily imply that the combustion process is highly inefficient; because a small  
428 amount of soot can absorb and scatter perceptible amounts of visible light, a flare with a  
429 combustion efficiency of 99 % could still smoke visibly (Castineira and Edgar, 2006).

430 **3.2 Emissions measurements around real-world gas flaring sites**

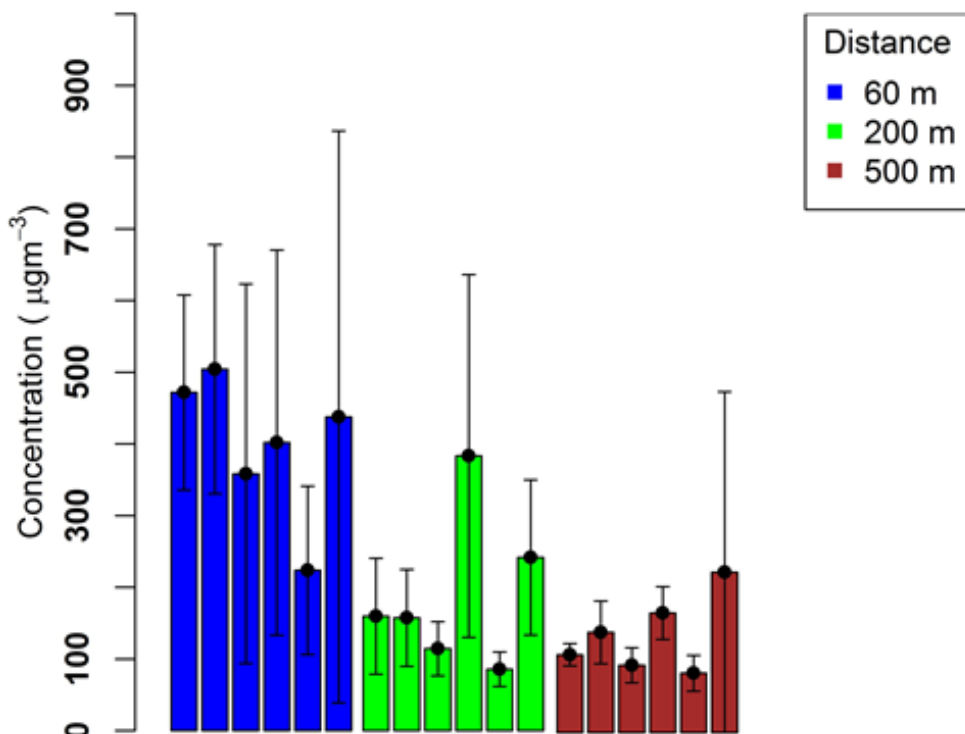
431 Few data of pollutants measurement around gas flaring sites are publicly available. Data from  
432 the ACCESS aircraft campaign experiment in the Arctic (Norway) and a couple of ground-  
433 based in-situ measurements in Nigeria and the US show significant contributions from gas  
434 flaring to ambient air concentrations of these pollutants.

435 In-situ ground measurements of air pollutants around typical oil and gas facilities where  
436 varying degrees of gas flaring take place have been undertaken in the US (Edwards et al.,  
437 2013; Edwards et al., 2014; Johansson et al., 2014), Mexico (Villasenor et al., 2003), Norway  
438 (Roiger et al., 2015) and, Nigeria (Ana et al., 2012; Nwaichi and Uzazobona, 2011;  
439 Obanijesu et al., 2009; Sonibare et al., 2010). Continuous noise levels higher than the WHO  
440 limit of 70 dB were also observed around some gas flaring sites in Nigeria (Abdulkareem and  
441 Odigire, 2006; Avwiri and Nte, 2004).

442 A 4-month sampling of three air pollutants (SO<sub>2</sub>, CO and NO<sub>2</sub>) around six flow stations in the  
443 Niger Delta area of Nigeria was undertaken by Obanijesu et al. (2009) and Sonibare et al.



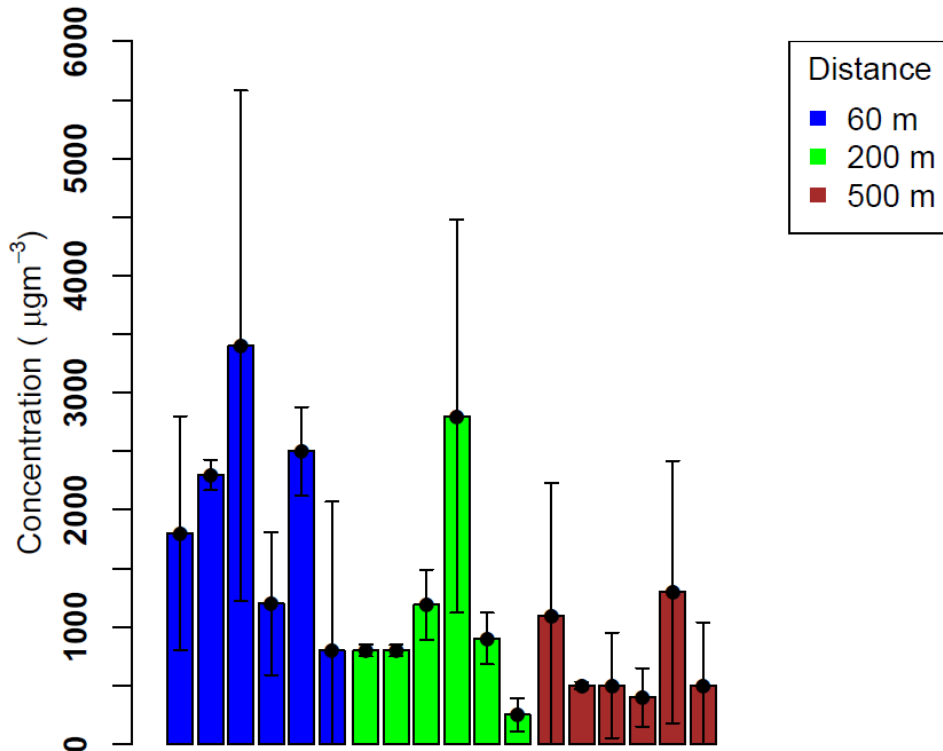
444 (2010). The measurements were made at 60, 200 and 500 m downwind of the flaring sites.  
 445 Although to a varying degree depending on the capacity of the station, gas flaring is a  
 446 prominent daily activity within the stations. Mean pollutants measurements around the six  
 447 flow stations are shown in Figures 6(a), (b) and (c). The variation bar on the bar-plots shows  
 448 the standard deviation of the measurements over the four-month period. The nature and  
 449 extent of dispersion of pollutants from a stationary source depend on the local meteorology  
 450 and topography of the area. As shown in Figures 6(a)-(c), the trend of the measurements from  
 451 the flaring sites are similar to observations from dispersion model studies where  
 452 concentrations of pollutants decreases exponentially with distance from the source (Hodgson  
 453 et al., 2007). Site 4 is the only place where a significant deviation from this trend, especially  
 454 for CO and NO<sub>2</sub>, was observed, suggesting the likelihood of contributions from other  
 455 source(s).



456 **Figure 6a:** Spatial variation of SO<sub>2</sub> concentration downwind of six gas flaring sites  
 457 (adapted from Obanijesu et al. (2009))  
 458

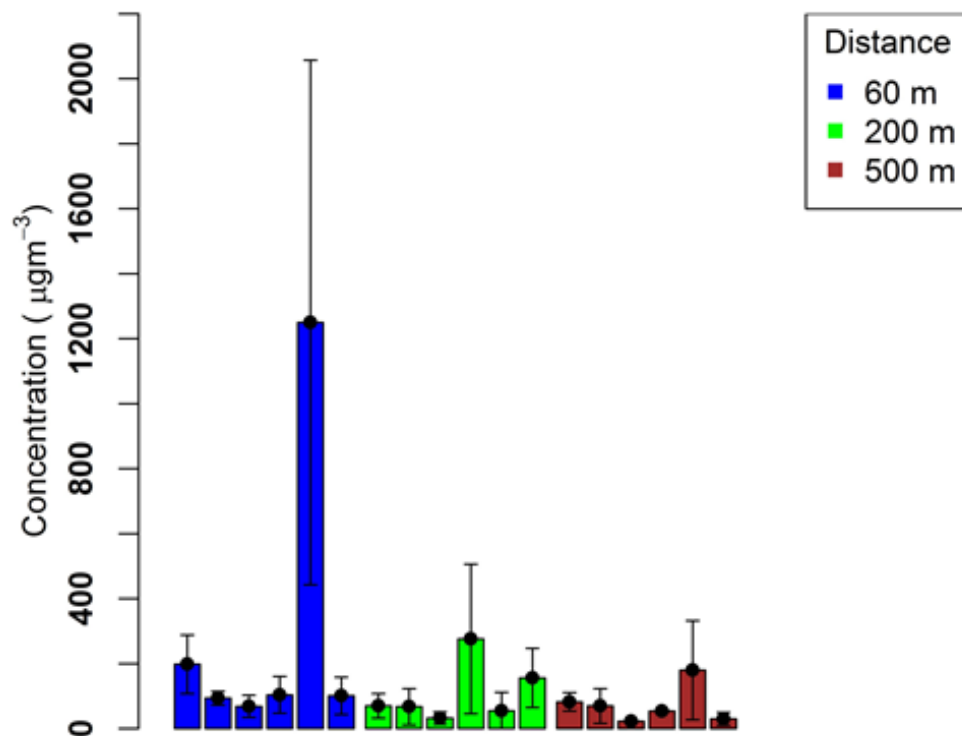
459  
 460  
 461

462



463  
464  
465

**Figure 6b:** Spatial variation of CO concentration downwind of six gas flaring sites (adapted from Sonibare et al. (2010))



466  
467  
468  
469  
470

**Figure 6c:** Spatial variation of NO<sub>2</sub> concentration downwind of six gas flaring sites (adapted from Sonibare et al. (2010))

471 A summary of the few available in-situ ground measurements downwind of gas flaring sites  
 472 in other regions of the world are given in Table 3.

473  
 474 **Table 3:** Pollutant measurements around several oil and gas facilities

BC (ng kg <sup>-1</sup> )	O <sub>3</sub> (ppbv)	VOC (ppbv)	PAH (ng m <sup>-3</sup> )	NO (ppbv)	NO <sub>2</sub> (ppbv)	SO <sub>2</sub> (ppbv)	CO (ppbv)	Ref
-	> 120	100 -350	-	> 3.5	> 7.5	-	> 80	Edwards et al. (2013)
> 40	> 25	-	-	> 1.2	-	> 1.2	> 90	(Roiger et al., 2015)
-	-	-	0.34 - 3.3x10 <sup>4</sup>	-	-	-	-	(Ana et al., 2012)

475  
 476

### 477 3.3 Types of Flares

478 Based on the design and operating condition of the system, flares can be categorised as *air-*  
 479 *assisted, steam-assisted, non-assisted* and *pressure-assisted*. Flares are assisted primarily to  
 480 enhance the turbulence and mixing of the fuel gas and air in the combustion zone, so as to  
 481 suppress smoking of the resulting flame (Castineira and Edgar, 2006; Enviroware, 2012;  
 482 Torres et al., 2012a). The choice of assistance, therefore, affects flame chemistry, as  
 483 discussed below. Air and pressure-assisted flares are not as efficient as steam-assisted flares  
 484 in terms of the carbon conversion efficiency (CCE) (Castineira and Edgar, 2006). Complete  
 485 combustion of the fuel gas requires sufficient air for combustion and adequate mixing of the  
 486 air and fuel gas. The efficiency of a gas flare at a given moment in time depends on the HHV  
 487 of fuel gas (see table 2), design of the burner, mixing of air and fuel gas in the combustion  
 488 zone, composition of the fuel gas, wind speed and direction, and ambient temperature and  
 489 pressure (Kostiuk et al., 2004; Stone et al., 1992; Torres et al., 2012b).

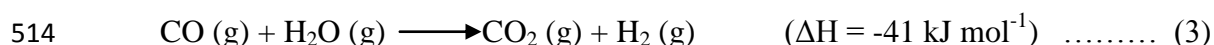
490 Equivalence ratio,  $\phi$ , is a measure of the amount of oxygen available for the combustion of  
 491 the fuel gas (Flagan and Seinfeld, 2012; McAllister et al., 2011). It is defined as:

492 
$$\phi = \frac{\left(\frac{A}{F}\right)_s}{\left(\frac{A}{F}\right)_a} \dots\dots\dots (2)$$

493 where  $\left(\frac{A}{F}\right)_s$  is the stoichiometric air-fuel mass ratio and  $\left(\frac{A}{F}\right)_a$  is the actual air-fuel mass ratio.  
494  $\phi < 1$  implies fuel-lean mixture, that is, more oxygen than is needed for the combustion of  
495 the fuel is available;  $\phi = 1$ , a stoichiometric mixture, where the exact amount of oxygen  
496 needed is made available, and  $\phi > 1$ , a fuel-rich mixture, less oxygen than is needed is  
497 available for the combustion of the fuel. Burners used in gas flaring and the entire gas flaring  
498 set-up are designed to produce a flame operating at  $\phi \sim 1$  taking into account the economic  
499 aspects such as cost effectiveness of applying a process like steam assistance.

### 500 3.3.1 Steam- Assisted Flare

501 Steam-assisted flare involves the introduction of steam jet into the combustion zone of the  
502 flare to provide added momentum and turbulence to the fuel gas and air, enhancing mixing  
503 and as such suppressing the tendency for smoke in the flare (Castineira and Edgar, 2006;  
504 Müller-Dethlefs and Schlader, 1976; Stone et al., 1992). It is the most efficient assist given to  
505 flare to suppress smoking during combustion because the steam affects flame chemistry as  
506 well as mixing. The steam acts to break up long-chain hydrocarbons to smaller chains that  
507 burn with less smoke (Castineira and Edgar, 2006; Fortner et al., 2012; Müller-Dethlefs and  
508 Schlader, 1976; Torres et al., 2012a). Steam undergoes thermal dissociation in a flare flame  
509 to give H and OH free radicals that react with carbon to give  $\text{CH}_2\cdot$  and  $\cdot\text{CHO}$  radical  
510 moieties. The steam-induced free radicals enhance the formation of C=O bonds rather than C-  
511 C bonds, promoting completeness of combustion. The steam can also react with intermediate  
512 products like CO, oxidizing it further to  $\text{CO}_2$  (Castineira and Edgar, 2006; Müller-Dethlefs  
513 and Schlader, 1976).



515 For a steam assisted flare, combustion efficiency starts to decrease when the steam-to-fuel  
516 gas ratio goes beyond a threshold which depends on the heat content of the fuel gas and the  
517 location at which the steam is injected into the combustion zone in the flare (USEPA, 2014).

518 In the US, a lower heating value (LHV) limit of 11.18 MJ/m<sup>3</sup> is imposed on fuel gas in order  
519 to be suitable for steam-assisted flares (Castineira and Edgar, 2006). Fuel gas with high heat  
520 content promotes higher combustion efficiency in steam-assisted flares (McDaniel and  
521 Tichenor, 1983; Torres et al., 2012b). Over-steaming results when too much steam is injected  
522 into the combustion zone; over-steaming is analogous to over-aeration in air-assisted flares.  
523 Over-steaming causes a decrease in the flame temperature by serving as a heat sink. A  
524 decrease in combustion efficiency of the flare results, along with, increased noise caused by  
525 cavitation created within the flame (Castineira and Edgar, 2006; Stone et al., 1992).

526 The formation of NO<sub>x</sub> in steam-assisted flares is reduced, compared to non-assisted flares,  
527 and further reduced at large values of equivalence ratio ( $\phi$ ) due to a drop in the flame  
528 temperature (Miyachi et al., 1981; Müller-Dethlefs and Schlader, 1976). Steam-assisted  
529 flares are rather expensive to maintain, especially for large gas facilities, as a large-scale  
530 steam generator is required.

### 531 **3.3.2 Air-Assisted Flare**

532 In air-assisted flares, forced air from a low-pressure blower is used as an additional source of  
533 momentum and turbulence to the fuel gas in the combustion zone and, hence, enhances the  
534 mixing of the fuel gas and air in the zone (Castineira and Edgar, 2006; Stone et al., 1992;  
535 Torres et al., 2012a). Air-assisted flaring involves the installation of an air blower that  
536 provides the forced air at the bottom of the stack. The major advantages of the air-assisted  
537 flare are that it is less expensive to run, extends the life-span of the flare by cooling the tip of  
538 the flare and is easier to maintain than other configurations (Castineira and Edgar, 2006). For  
539 an air-assisted flare, the combustion efficiency of the flare decreases linearly above a  
540 threshold limit of the air assist to fuel-gas ratio, but the rate of decrease is slow for a fuel gas  
541 with a higher VHV (Torres et al., 2012b). Incomplete combustion can occur when air-fuel

542 gas ratios go beyond the optimum value, to the extent that the flame may be put out as a  
543 result of over-aeration (Castineira and Edgar, 2006).

### 544 **3.3.3 Pressure-Assisted Flare**

545 In pressure assisted flares, the fuel gas stream pressure is controlled by varying the volume  
546 flow of the fuel gas, and used to enhance the mixing of the fuel gas and air in the combustion  
547 zone. A high-pressure burner is used to promote atomization of any liquid hydrocarbon and  
548 enhance the mixing of the fuel gas with air to bring about a complete or near-complete  
549 combustion. Pressure assistance often requires significant amount of space in a remote area  
550 because of the burners arrangement at ground level. Fuel gas exit velocity increases with  
551 pressure at the burner. Pressure-assisted flares usually have burners arranged on the ground  
552 and as such must be located carefully within the oil and gas production plant (Enviroware,  
553 2012; Stone et al., 1992).

### 554 **3.3.4 Non-Assisted Flare**

555 For non-assisted flares, no provision is given to provide momentum and enhanced mixing for  
556 the fuel gas and air. The method is often used for gases with low VHV, that is, fuel gas  
557 having low C-to-H ratio (in alkanes, C-to-H ratio increases from a minimum value of 0.25 for  
558 methane; see Table 2). The C-to-H ratio determines the smoking tendency of hydrocarbons,  
559 with smokiness increasing with C-to-H (USEPA, 1995). Note that the experimental fuel gas  
560 compositions listed in Table 2 are at or below the lowest C-to-H ratio of the Flow Station gas  
561 compositions listed. Non-assisted flaring is used for gases that require smaller amounts of air  
562 to undergo complete combustion (Enviroware, 2012; Stone et al., 1992).

563 Table 4 summarises the features of the different types of flares discussed in Section 3.3.

564

565

**Table 4:** Summary of the properties of flare types

	<b>Steam-assisted</b>	<b>Air-assisted</b>	<b>Pressure-assisted</b>	<b>Non-assisted</b>
<b>Method</b>	Steam is introduced into the combustion zone to enhance mixing.	Air is introduced from a blower to enhance the mixing and turbulence of the fuel gas in the combustion zone	The vent pressure of the gas flow is used to enhance mixing at the tip of the flare burner	No assistance is given to the combustion process
<b>Efficiency</b>	Most efficient in terms of suppressing soot formation. Some of the CO formed can be oxidized to CO <sub>2</sub>	Less efficient than the steam assisted flare but relatively efficient that the other two types	Not as efficient as steam and air-assisted but can equally suppress sooting.	Only efficient for non-sooting combustion especially in light hydrocarbons
<b>Benefits</b>	Fuel with high heat value, and hence, high sooting propensity can be disposed of with relatively less soot	Prolongs the life span of the flare tip. Less expensive than steam-assisted and easy to maintain, hence, it is the most commonly used.	Enhance combustion efficiency when the gas flux pressure is sufficiently high enough without the additional cost of steam and air generation	Can be used for occasional emergency flaring of near smokeless gas
<b>Relative size</b>	They are often large flares as they include the steam generator and are usually employed in large gas facilities.	Not as large as the steam assisted.	May be of same size as air-assisted flare depending on the flow capacity of the facility	Often smaller in size compared to the other types
<b>Shortcoming</b>	Over-steaming can result in reduced efficiency of flare. It is also expensive to maintain on a large-scale	Over- aeration can also result in less efficiency. A limit of air assist to gas ratio must be maintained for effectiveness of the flare.	The fluctuation of gas flow pressure has a bearing consequence on the efficiency of the combustion. Requires large space in a remote area.	Cannot be used for dense fuels with high sooting propensity which are typical gas in oil and gas processing facilities

## 568 **4 Estimating emissions from gas flaring**

569 Emissions from a typical gas flare can be solids, liquids or gases. As a result of the  
570 inaccessible nature of full-scale real-world gas flares, several techniques have been used to  
571 quantify the amount of emissions from such flares. Such methods include measurement or  
572 source monitoring often by lab-based, pilot-study-based or field-based study (Johnson et al.,  
573 2011; McEwen and Johnson, 2012), application of emission factors obtained from  
574 measurements and scaling calculations (Giwa et al., 2014; Huang et al., 2015; Sonibare and  
575 Akeredolu, 2004; Talebi et al., 2014; USEPA, 1995) and, simulations, often by computational  
576 fluid dynamics (CFD) (Almanza et al., 2012).

577 In real-world flares, complete combustion cannot be achieved always and everywhere.  
578 Incomplete combustion of the fuel gas can be due to poor efficiency of the flare system,  
579 flame temperature (flame dynamical characteristics), insufficient oxygen resulting in poor  
580 stoichiometric air/fuel gas mixing ratio, the condition of the fuel gas in the combustion zone  
581 and prevailing ambient meteorological condition (Stone et al., 1992). Carbon monoxide (CO)  
582 can represent 24 – 80 % (on carbon a molar basis) of emissions for an incomplete combustion  
583 process (Torres et al., 2012b).

### 584 **4.1 Determining the flame regime**

585 It is important to define clearly the configuration of the fire (flare) as this is essential for an  
586 adequate estimation of the yield and transport of pollutant species from the combustion  
587 process. Flames can be classified along a spectrum ranging from turbulent diffusion flames  
588 (of the kinds discussed above) to pool fires (e.g. tar-pool fire) based on the nature and  
589 dynamics of the fuel in the flame as well as the design of the burning process (Delichatsios,  
590 1987, 1993a). In this review we are concerned with gas flares, which are classified as  
591 turbulent jet-diffusion flames. They are so classified because of the high pressure associated  
592 with the release of the fuel gas into the flame.



593 Jet-diffusion flames in the environment can be categorized based on the momentum flux  
594 ratio,  $R$ , of the jet plume versus the horizontal momentum flux of the ambient wind (Huang  
595 and Wang, 1999). Flares with high  $R$  ( $R > 10$ ) may be further categorized depending on  
596 whether the flame characteristics are driven by the buoyancy of the hot plume or momentum  
597 of the fuel gas (McEwen and Johnson, 2012). Both buoyancy and momentum are important  
598 in determining the character of flares. A combination of several dimensionless parameters –  
599 Richardson number, Richardson ratio, fire Froude number, gas Froude number, and Reynolds  
600 number - have been used in studies to configure the regime of the flame in a jet-diffusion  
601 flame. The Froude numbers measure the ratio of the inertia force on an element of the fluid  
602 (in this case, gas or fire) to the weight of (i.e. gravitational force acting on) the fluid element.  
603 The fire Froude number,  $Fr_f$ , gas Froude number,  $Fr_g$  and Reynolds number,  $Re$ , have  
604 proved to be useful dimensionless parameter to define the flame regime (Becker and Liang,  
605 1982; Delichatsios, 1993a; Delichatsios, 1993b; Delichatsios, 1987; Sivathanu and Faeth,  
606 1990).

607 
$$Fr_g = \frac{u_e f_s^{3/2}}{(g d_e)^{1/2} \left(\frac{\rho_e}{\rho_\infty}\right)^{1/4}} \dots\dots\dots (4)$$

608 
$$Fr_f = \frac{u_e f_s^{3/2}}{\left(\frac{\Delta T_f}{T_\infty} g d_e\right)^{1/2} \left(\frac{\rho_e}{\rho_\infty}\right)^{1/4}} \dots\dots\dots (5)$$

609 
$$Re_s = \frac{u_e d_e}{\nu_o} \dots\dots\dots (6)$$

610 
$$f_s = \frac{1}{s+1} \dots\dots\dots (7)$$

611 In the definition of  $Fr_f$  in equation (5),  $\left(\frac{\Delta T_f}{T_\infty}\right) g$  is the effective acceleration generated by  
612 individual hot eddies burning at the flame temperature (Delichatsios, 1987). Among the three  
613 dimensionless numbers defined by equations (4) - (6), the Reynolds number is used to

614 determine the status of flow, either turbulent or laminar. The fire Froude number,  $Fr_f$ , is used  
615 to identify the dominant mechanism between buoyant-generated turbulence and momentum-  
616 generated turbulence. In practice,  $Fr_f$  can be used to parameterise soot yield from turbulent  
617 diffusion flames (Delichatsios, 1993b; McEwen and Johnson, 2012).

#### 618 **4.2 Emission factors (EF) for gas flaring emissions**

619 The Emission factor (EF) of a pollutant is the amount of the pollutant released into the  
620 atmosphere per unit activity or per unit raw material consumed. It can be obtained from  
621 experimental measurements carried out on several sources which represent a particular  
622 emission source type. For example, road transport emission factor can be compiled by  
623 measuring the amount of each pollutant ( $\text{CO}_2$ , CO, PM,  $\text{NO}_x$ ) given off by cars (petrol and  
624 diesel), heavy duty vehicles and motorbikes per litre of fuel burned for every km travelled  
625 (Gertler et al., 1998; USEPA, 1995; Zhang and Morawska, 2002) under given driving  
626 conditions. It is often expressed in  $\text{g m}^{-3}$  (pollutant produced per unit volume of raw material  
627 consumed),  $\text{g kg}^{-1}$  (pollutant produced per unit mass of raw material consumed),  $\text{g km}^{-1}$   
628 (pollutant produced per unit distance travelled). Emission factors have been compiled by  
629 several agencies, which include the US Environmental Protection Agency (USEPA), the  
630 European Environmental Agency (EEA), the United Kingdom Department for Environment,  
631 Food and Rural Affairs (Defra), and GAINS (Greenhouse gas Air Pollution Interactions and  
632 Synergies), for several source categories based on technical sessions of lab-based studies,  
633 pilot studies or actual field measurements. Of these agencies, ECLIPSE and USEPA have  
634 EFs specifically for emissions from gas flares: the GAINS emission factor for BC from gas  
635 flaring is  $1.6 \text{ g m}^{-3}$ ; the equivalent USEPA value has four discrete values between 0 and  $6.4 \text{ g}$   
636  $\text{m}^{-3}$  depending on the smokiness of the flame (see below). Stohl et al. (2013) in their study  
637 used emission factor of  $1.6 \text{ g m}^{-3}$  obtained from ECLIPSE (Evaluating the Climate and Air

638 Quality Impacts of Short-lived Pollutants) emissions data set to simulation BC emissions in  
639 the Arctic.

640 It is difficult to carry out an accurate estimate of emission from gas flares directly from field  
641 measurements. Conventional experimental techniques are not suited due to the severe  
642 operating conditions that occur in the flaring process and the almost uninhabitable nature of  
643 the gas flaring area to both man and the field equipment during the process of gas flaring  
644 (Ismail and Umukoro, 2014; McDaniel and Tichenor, 1983; McEwen and Johnson, 2012;  
645 RTI, 2011; Talebi et al., 2014). As a result of the unsteady and opaque nature of gas flare  
646 flames, remote sensing provides only a partial answer to the difficulties of in-situ monitoring.

647 In Chapter 13 of USEPA's 5<sup>th</sup> edition of the compilation of air pollutant emission factors  
648 known as AP-42, published in January 1995, emission factors (EF) for pollutant emitted from  
649 industrial flaring of waste gas were given; these were recently updated in 2014 (though still  
650 in the draft stage) except those for soot. The EFs published in 1995 were based on a study  
651 conducted by McDaniel and Tichenor (1983) aimed at determining combustion efficiency  
652 and hydrocarbon destruction efficiency for flares operated under different condition. The  
653 recent updates of EFs in AP-42 give emission factors of 0.17 kg GJ<sup>-1</sup>, 1.43 kg GJ<sup>-1</sup> and 0 - 6.4  
654 g m<sup>-3</sup> are given for CO, NO<sub>x</sub> and soot, respectively.

655 The fuel used in the pilot study to estimate EFs for industrial flare pollutants in the AP-42  
656 compilation was predominantly propylene and inert diluents. As such, the EFs, especially for  
657 soot, might not be an adequate representation of a typical flare in the oil and gas industry with  
658 varying fuel gas composition (Table 2). For AP-42, the collection of soot at the experimental  
659 stage was not done by a conventionally accurate method. For instance, the particulate matter  
660 (soot) given off was not collected isokinetically in accordance with USEPA's method 5 for  
661 sampling particulate matter from stationary source (USEPA, 2000). An emission factor of 0.0

662  $\mu\text{g L}^{-1}$  (microgram per litre of fuel gas at standard temperature and pressure) given for soot in  
663 non-smoking flares of industrial flares in AP-42 is of limited utility and presumably denotes a  
664 upper limit of  $0.05 \mu\text{g L}^{-1}$ , because the soot yield from flares is never likely to be precisely  
665 zero. Even seemingly modest emission of soot (BC) can be significant, given what is now  
666 known of the effects of BC on climate, weather and human health from findings in recent  
667 studies (Bond et al., 2013; Ramanathan and Carmichael, 2008; Stocker et al., 2013; Tripathi  
668 et al., 2005; Wang et al., 2014).

669 The mass/mole balancing technique for estimating the yield of pollutants from the  
670 combustion of hydrocarbon is a widely used technique. Using this technique, Ismail and  
671 Umukoro (2014) and Sonibare and Akeredolu (2004) estimated the yield for  $\text{SO}_2$ ,  $\text{NO}_x$ ,  $\text{CO}_2$   
672 and CO from the combustion of fuel gas (hydrocarbon with inert diluents) at various levels of  
673 combustion. Both studies did not account for unburned carbon (soot) even for their ‘severely’  
674 incomplete combustion process reactions. Ismail and Umukoro (2014) varied combustion  
675 efficiency (CE) and air available for combustion, and with CE as low as 0.5 (50 %) still did  
676 not account for unburned carbon.

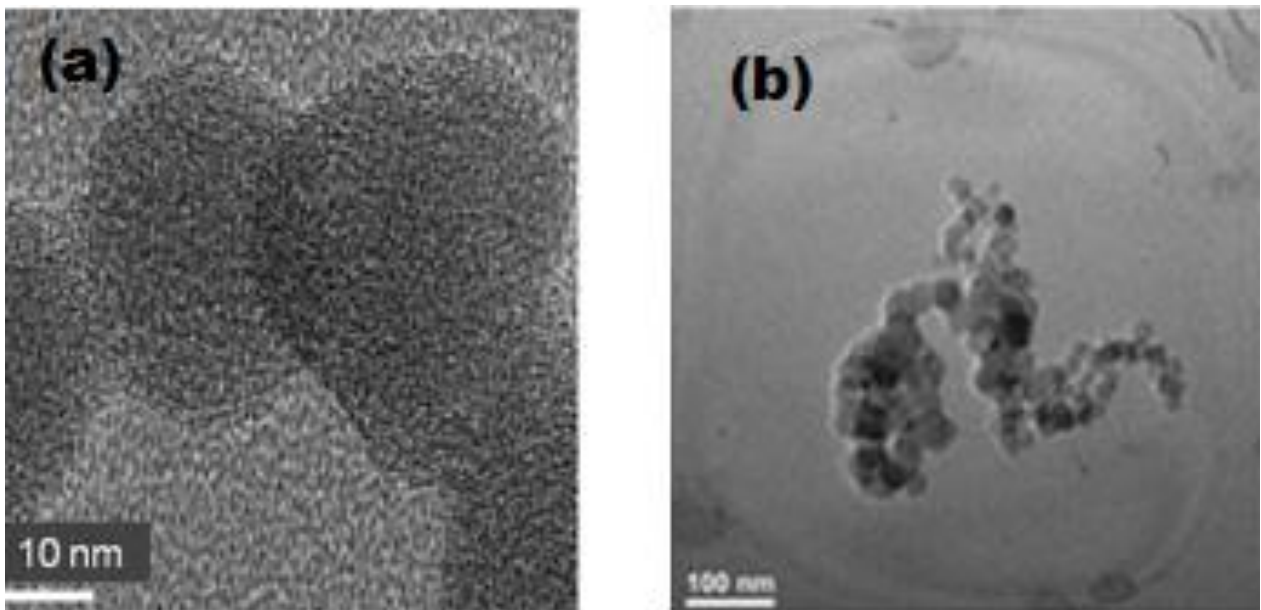
### 677 **4.3 Soot emission from gas flaring**

678 Soot, which is predominantly black carbon (BC), is a product of the incomplete combustion  
679 of biomass, solid fuel and fossil fuel (Goldberg, 1985; Koch et al., 2009). Globally, fossil fuel  
680 combustion is estimated to contribute 3 Mt of BC to the atmosphere annually (Bond et al.,  
681 2004). Annually, the contribution of gas flaring to global BC concentration is estimated to be  
682 260 Gg (Bond et al., 2013), that is approximately 0.1% of the total contribution from fossil-  
683 fuel use, of which Russia is estimated to contribute 81.0 Gg (Huang et al., 2015).

684 The formation and quantification of soot from the combustion of hydrocarbon is a rather  
685 complex thermo-chemical process that is not well understood, despite decades of research

686 (Castineira and Edgar, 2006; Haynes and Wagner, 1981; Johnson et al., 2011; Maricq, 2009).  
687 Soot given off from the combustion of hydrocarbon is predominantly elemental carbon and  
688 the amount given off depends on a number of factors, including the efficiency of the  
689 combustion process and the fire dynamical characteristics.

690 The diameter of soot particles emitted ranges between 10 – 200 nm and most commonly lies  
691 between 10 and 50 nm. Figure 7 shows a TEM micrograph of soot particle and agglomerates  
692 from acetylene flames. The very fine particle of soot are from seemingly 'non-sooting' flames  
693 while at the other extreme are those from heavily sooting flames (Flagan and Seinfeld, 2012;  
694 Glassman, 1996; Haynes and Wagner, 1981). Combustion of hydrocarbon components of the  
695 fuel gas has PAH and BC signatures which can be used as tracers for emissions from the  
696 flaring of fuel gas (Fortner et al., 2012; Maricq, 2009).



697 **Figure 7:** TEM micrograph of soot (a) microstructure (b) agglomerates (Tumolva et al.,  
698 2010).  
699

700

701 Soot is formed when the carbon particles are cooled below their ignition temperature and  
702 there is a deficiency of oxygen (Stone et al., 1992). Considering the variation of the

703 composition of gas flared from one station to the other, EFs available for estimating  
 704 emissions from gas flares are overly generalised. The fuel gas used in most of the studies to  
 705 estimate the EFs is either propylene or propane or a mixture of both with nitrogen added to  
 706 alter the heat content as well as the use of predominantly methane-based fuels which are  
 707 known to be low-sooting.

708 Several attempts have been made to quantify and study the characteristics of soot yield from  
 709 gas flares using various approaches in lab-based, pilot-based and field-based studies as well  
 710 as simulation techniques. Emission factors from some of these studies are given in Table 5.  
 711 Other emission factors not highlighted in this table are based on the USEPA's AP-42  
 712 emission factors.

713  
 714

715 **Table 5:** A Summary of Emission Factors/Emission rate for Soot from Industrial Flares

Study (year)	Emission factor (g m <sup>-3</sup> of fuel burned)	Emission rate (g s <sup>-1</sup> )	Type of study	Fuel
USEPA (1995)	0.0, 0.9, 4.2 6.4 <sup>a</sup>	-	Pilot study	80% propylene 20% propane
Johnson et al. (2011)	-	2.0 (±0.66)	Field study	associated natural gas
Almanza et al. (2012)	-	0.025 – 0.22	CFD simulation	associated natural gas
McEwen and Johnson (2012)	0.51	-	Lab-scale flare	hydrocarbon (alkanes)
Johnson et al. (2013)	-	0.067	Field study	-
GAINS 2011	1.6	-	Modelling	-
IMP (2006) <sup>b</sup>	-	3.37	Simulation	associated natural gas
CAPP (2007)	2.563	-	-	associated natural gas

716 <sup>a</sup>0.0 is for *non-smoking* flame, 0.9 for *light smoking* flares, 4.2 for *averagely smoking* flare  
 717 and 6.4 for *heavily smoking* flares

718 <sup>b</sup> cited in (Almanza et al., 2012)

719

720 The studies by Johnson et al. (2011) and Johnson et al. (2013) gave emission rates (g s<sup>-1</sup>) and  
 721 not emission factors (g m<sup>-3</sup>) because both were actually field studies that quantified the soot

722 given off per unit time by estimating the travel (speed) of the soot in space using a charge  
723 couple device camera (CCD) camera viewing a real field flare.

724 Emission of soot from the combustion of hydrocarbon varies with the VHV of the gas and, as  
725 such, the emission factor for soot can be estimated from its VHV (McDaniel and Tichenor,  
726 1983; RTI, 2011; Torres et al., 2012b). McEwen and Johnson (2012), using a lab-based  
727 experiment, studied the BC emission from the combustion of hydrocarbon. The study varied  
728 the VHV of the fuel gas and measured the soot yield for each combustion process. The VHV  
729 used here is the higher heating value (HHV), or gross heating value. The relationship between  
730 the two variables (soot yield and HHV) obtained from the study by McEwen and Johnson  
731 (2012) is given in equation (8):

732 
$$EF_{soot} = 0.0578(VHV) - 2.09 \dots\dots\dots (8)$$

733 When the composition of the fuel gas is known, its VHV can be calculated from standard  
734 thermochemical tables (cf. Table 2). It should, however, be noted that because the VHV  
735 contains no information on flame dynamics, this relationship is only appropriate for the flame  
736 dynamics conditions of the experiment. Although, equation (8) is a readily available  
737 relationship to estimate soot emission from hydrocarbon combustion, its application is  
738 restricted to a complete or near-complete combustion process. Inserting the estimated VHV  
739 into the relation developed by McEwen and Johnson (2012) gives an estimate of the soot  
740 yield in  $\text{g m}^{-3}$ .

741 **4.4 Scaling soot emission from lab-based studies**

742 Lab-based studies of emissions from flares are the most common and readily available  
743 method to estimate emissions from full-scale flares. However, considering the size (diameter)  
744 of the flare stack, flow rate of fuel gas, exit velocity, and the resultant buoyancy of full-scale  
745 flare, there is a need to scale up the emissions yield from lab-based studies to be  
746 representative of a full scale flare. In earlier studies, several dimensionless parameter have

747 been considered for such scaling purpose; these include Richardson ratio,  $Ri_L$  (Becker and  
 748 Liang, 1982), fire Froude number,  $Fr_f$  (McEwen and Johnson, 2012), and the first  
 749 Damköhler ratio,  $Da_l$  (Becker and Liang, 1982). Richardson ratio,  $Ri_L$ , is defined as the ratio  
 750 of the buoyancy-generated turbulent kinetic energy (TKE) of the flame to the TKE of emitted  
 751 gas jet at the exit:

$$752 \quad Ri_L = \frac{gL^3}{(u_e d_e)^2} \left( \frac{\rho_\infty}{\rho_e} \right) \dots\dots\dots (9)$$

753 Richardson ratio is the basis to assess the turbulent regime of the flame: when  $Ri_L \ll 1$ ,  
 754 buoyancy-induced mixing between emitted gas jet and background air is much weaker than  
 755 jet-induced mixing, and consequently the flame is dominated by forced convection; when  
 756  $Ri_L \gg 1$ , jet-induced mixing is much weaker than buoyancy-induced mixing and the flame is  
 757 dominated by natural convection. Fire Froude number,  $Fr_f$ , is defined in Equation (5) and can  
 758 be interpreted as the ratio of the jet’s inertia to the buoyancy force acting on it. Fire Froude  
 759 number can be used to assess the dominating force to “stretch” the flame: when  $Fr_f \gg 1$ , the  
 760 jet’s momentum is the dominating factor and when  $Fr_f \ll 1$ , the flame’s buoyancy force is  
 761 the dominating factor. Comparing  $Fr_f$  against  $Ri_L$ , we understand that both are used to assess  
 762 the dominating factor between jet-related quantity and buoyancy-related quantity, but there  
 763 are two differences: (1) the quantity is momentum ( $\propto$  velocity) for  $Fr_f$ , but TKE ( $\propto$  velocity  
 764  $\times$  velocity) for  $Ri_L$ ; (2) the ratios between jet-related quantity and buoyancy-related quantity  
 765 are reciprocal:  $Ri_L \propto$  (buoyancy-related quantity)/( jet-related quantity) whereas  $Fr_f \propto$  (jet-  
 766 related quantity)/( buoyancy -related quantity). Therefore, these two parameters are closely  
 767 related and mathematically their relationship should be  $Ri_L \propto Fr_f^{-2}$ . Precise relationship  
 768 between them can be derived from Equations (5) and (9):

$$769 \quad Ri_L = \left( \frac{\rho_\infty}{\rho_e} \right)^{3/2} \left( \frac{L}{d_e} \right)^3 \left( \frac{T_\infty}{\Delta T_f} \right) \cdot f_s^3 \cdot Fr_f^{-2} \dots\dots\dots (10)$$



770 It is noted that  $\left(\frac{L}{d_e}\right)^3$  can be interpreted as the volume expansion ratio of the flaring gas due  
 771 to burning and  $\left(\frac{T_\infty}{\Delta T_f}\right)^{-1}$  can be approximated as the temperature rising ratio of the flaring gas  
 772 due to burning. Based on the gas law, these two are proportional to each other for an isobaric  
 773 process (from the exit to the flame tip) which is a good assumption for gas flaring, i.e.  
 774  $\left(\frac{L}{d_e}\right)^3 \propto \left(\frac{T_\infty}{\Delta T_f}\right)^{-1}$ , or equivalently,  $\left(\frac{L}{d_e}\right)^3 \left(\frac{T_\infty}{\Delta T_f}\right) \approx \text{const}$ . Therefore, Equation (10) confirms  
 775 the relationship of  $Ri_L \propto Fr_f^{-2}$ . This suggests a strong dependence between adopting  $Ri_L$  and  
 776 adopting  $Fr_f$  as the scaling parameter.

777 The first Damköhler ratio,  $Da_1$ , however, is defined as the ratio of residence time of fuel in  
 778 flame ( $\tau_{res}$ ) to chemical time of burning process ( $\tau_{chem}$ ):

779 
$$Da_1 = \frac{\text{residence time in flame, } \tau_{res}}{\text{chemical time, } \tau_{chem}} = \left(\frac{L}{u_e}\right) / \tau_{chem} \dots\dots\dots (11)$$

780 It describes the extent of the oxidation process within the flame in relation to the oxidant's  
 781 feed rate. For a large  $Da_1$  (i.e.  $\tau_{res} \gg \tau_{chem}$ ), the velocity fluctuating component does not  
 782 have much influence on the chemistry of the flame. The chemical reaction is able to proceed  
 783 to completion within the residence time in the combustion zone, resulting in intensive  
 784 chemical reaction and hot diffusion flame. For a small  $Da_1$  (i.e.  $\tau_{chem} \gg \tau_{res}$ ), turbulence  
 785 can significantly affect the chemistry and structure of the flame. The rate of chemical reaction  
 786 and hence, heat release may be affected, causing combustion product to be mixed with  
 787 reactants within a time interval shorter than the chemical reaction time (Lieberman, 2010;  
 788 William, 1985). From the perspective of processes,  $Da_1$  involves an extra dimension (i.e.  
 789 chemical processes) which is not reflected by either  $Ri_L$  or  $Fr_f$ . In principle, we should  
 790 consider  $Da_1$  as one more scaling parameter.

#### 791 **4.5 Soot modelling**

792 Mathematical modelling is a technique that has been used by scientist and engineers over the  
793 years to understand the relationship between sets of input and output parameters in a process,  
794 especially where the 'real world' process is often remote or grossly complicated to assess. The  
795 region of validity of such model outputs is often limited as several assumptions and constants  
796 are applied in the modelling to further simplify the process being studied.

797 Soot formation and oxidation in pre-mixed and non-premixed (diffusion) hydrocarbon flames  
798 have been studied using several modelling techniques including computational fluid  
799 dynamics (CFD). The main problem with mathematical modelling of turbulent combustion of  
800 hydrocarbon is the problem of modelling turbulent flow and chemical kinetics and the  
801 interaction between flow and chemical reaction (Magnussen and Hjertager, 1977). Kennedy  
802 (1997) classified the models for soot formation as empirical correlations, semi-empirical  
803 correlation models and models with detailed chemistry and physics of soot formation. The  
804 flame temperature, C:H ratio and number of carbon atoms in the fuel (hydrocarbon) are  
805 important parameters considered to have strong influence on the sooting propensity of the  
806 hydrocarbon (Harris et al., 1986). These parameters have been the basis of measurements  
807 used in most empirical correlation models.

808 In their study to modelling soot formation and combustion, Magnussen and Hjertager (1977)  
809 assumed that soot is formed from a gaseous hydrocarbon in two stages (a) formation of  
810 radical nuclei, and (b) soot particle formation from these nuclei. Applying expressions for the  
811 rate of formation of radical nuclei and rate of soot particle formation expressions developed  
812 by Tesner et al. (1971a); (Tesner et al., 1971b) in their model, tested on both pre-mixed and  
813 diffusion flame, they predicted soot concentrations that are in close agreement with  
814 experimental data. They concluded that soot formed and was contained in eddies and burned  
815 away during turbulence dissipation.

816 Moss et al. (1989), using a two-equation model for the evolution of soot volume fraction and  
 817 number density, simulated the formation of soot. They included the influences of nucleation,  
 818 surface growth and coagulation on the rate of soot formation. As given in equations 12(a) and  
 819 (b), their model contains simplified expressions to quantify particle nucleation, growth and  
 820 coagulation; using three empirical constants that are dependent on the fuel to control the rate  
 821 of these processes. A major finding from their study is that soot volume fraction is  
 822 proportional to the square of pressure.

823 
$$\left\{ \frac{d\left(\frac{n}{N_0}\right)}{dt} \right\} = \alpha(\zeta) - \beta(\zeta)\left(\frac{n}{N_0}\right)^2 \dots\dots\dots 12(a)$$

824 
$$\rho_s \left\{ \frac{df_v}{dt} \right\} = \gamma(\zeta)n + \delta(\zeta) \dots\dots\dots 12(b)$$

825 where  $\rho_s$  is the assumed density for solid carbon ( $1.8 \times 10^3 \text{ kgm}^{-3}$ ),  $N_0$  is Avogadro's number  
 826 and  $\zeta$  is the mixture fraction. Rates of the processes are expected to be a function of the  
 827 mixture fraction. The rates of the processes are defined explicitly in terms of the fuel density,  
 828  $\rho$ , temperature,  $T$ , and fuel mole fraction,  $X_c$  as described in equation 13:

829 
$$\left. \begin{aligned} \alpha &\equiv C_\alpha \rho^2 T^{1/2} X_c \exp\left(-T_\alpha/T\right); \beta \equiv C_\beta T^{1/2} \\ \gamma &\equiv C_\gamma \rho T^{1/2} X_c \exp\left(-T_\gamma/T\right); \delta \equiv C_\delta \alpha \end{aligned} \right\} \dots\dots\dots 13$$

831 coefficients  $C_{\alpha,\beta,\gamma,\delta}$  and activation temperatures,  $T_\alpha$  and  $T_\gamma$  are obtained from experimental  
 832 data. In equations 12(a), the first and second term on the left are nucleation and coagulation  
 833 processes, respectively. And, in equation 12(b), the first and second term on the left represent  
 834 the growth and nucleation, respectively.

835 Lautenberger et al. (2005) developed a CFD model to study the formation and oxidation of  
836 soot. Since their model was to generate enough accurate predictions of soot emission  
837 concentrations in order to estimate CFD simulations of fire radiation from turbulent flames,  
838 considerations were given only to phenomena which were essential. Soot estimation in their  
839 model was based on a further simplified form of the two-equation model of Moss et al.  
840 (1989). There are no fuel-specific constants in their estimations, but rather, they used the  
841 laminar smoke point height to account for the sooting propensity of different fuels. The  
842 smoke point of a flame is its length just before the onset of the release of visible smoke.  
843 Length of a flame is dependent on the extent of completeness of the combustion and heat  
844 content of the fuel gas (Beychok, 1994).

845 The use of CFD simulation soot has made it possible to make predictions about the  
846 relationships between the various processes involved in soot formation and oxidation in both  
847 pre-mixed and diffusion hydrocarbon flames as well as the sensitivity of the soot formation to  
848 some of the complex phenomena. However, the veracity of CFD simulation results is limited  
849 by the availability of field measurements for model evaluation.

#### 850 **4.6 Gas flaring emissions in global models and inventories**

851 To the best of our knowledge, the only two emission datasets that explicitly includes gas  
852 flaring emissions are EDGAR (Emissions Database for Global Atmospheric Research) and  
853 ECLIPSE (Evaluating the Climate and Air Quality ImPacts of Short-livEd Pollutants)  
854 gridded emissions datasets.

855 In EDGAR v4.2, for gas venting and flaring, emissions were calculated for 1994 onwards  
856 using the amount of gas flared estimated from satellite observations of intensities of light  
857 from various gas flares. The estimated quantities of gas flared and emission factors obtained  
858 from either inventory guidance documents or confidential information were used to generate

859 gridded annual emission datasets for different countries on a resolution of  $0.1^\circ \times 0.1^\circ$ . In  
860 2005, the inclusion of new primary data sources for gas flaring in EDGAR v4.2 gives rise to  
861 a change of +75 % of EDGAR 4.1 value (130 Tg) in global CO<sub>2</sub> emission (European  
862 Commission, 2009).

863 ECLIPSE is provided by the IIASA (International Institute for Applied Systems Analysis).  
864 Emission calculations for the historical years (2005 – 2010) were developed in a series of  
865 regional and global projects. For gas flaring, emissions were calculated using data available  
866 from NOAA, NASA and the World Bank collaborative work to estimate the volume of gas  
867 flared globally. The volume of gas flared was estimated using NASA MODIS active fire  
868 detection products (Elvidge et al., 2007; Elvidge et al., 2011). Emission factors and other  
869 parameterizations were obtained from peer-reviewed data on emission performance of  
870 various technologies. The calculation was performed with the IIASA GAINS model (Klimont  
871 et al., 2013). The ECLIPSE v4 global emission dataset is available on a  $0.5^\circ \times 0.5^\circ$  lon-lat  
872 resolution.

873 Stohl et al. (2013), performing a 3-year black carbon (BC) simulation in the Arctic, using a  
874 Lagrangian particle dispersion model FLEXPART driven by the ECLIPSE dataset, estimated  
875 that more than 40 % of mean surface BC surface concentration in the Arctic is attributable to  
876 gas flaring. Although, more studies on the sensitivity of global models to gas flaring emission  
877 is needed to give a clear and precise quantification of the contribution of gas flaring emission  
878 to global aerosol loadings, the change in global CO<sub>2</sub> level in EDGAR4.2 underscores the  
879 importance of an explicit inclusion of gas flaring emissions in global models.

## 880 **5 Conclusion**

881 The World Bank has been at the fore-front of the campaign to reduce gas flaring through the  
882 public-private partnership project “Global Gas Flaring Reduction (GGFR)”

883 (<http://www.worldbank.org/en/programs/gasflaringreduction>). The “Zero Routine Flaring by  
884 2030” initiative was launched in April 2015 by the World Bank, United Nations,  
885 governments and oil companies. As at April 17 2015, a total of nine countries have agreed to  
886 the “Zero Routine Flaring by 2030” initiative. At the time of writing, some major flaring  
887 nations have yet to sign up to the initiative. Indeed, some major flaring countries still struggle  
888 to meet targets for gas flaring set in the late 1980s. A steep increase in flaring since 2006 has  
889 been reported for the USA and Canada, associated, presumably, with the exploitation of  
890 unconventional hydrocarbon reservoirs.

891 Considering the wide spectrum, quantity and effects of pollutants emitted from gas flaring,  
892 coupled with the estimated quantity of gas flared globally, it is surprising that so little effort  
893 has been put into adequately understanding the yield of pollutants, especially BC, from the  
894 process in real world field situations. The wide variation of fuel gas compositions from flow  
895 stations around the world underpins the importance of developing strategies that take these  
896 compositions into consideration when estimating emissions.

897 The steep decrease in the fraction of total gas production flared between 2000 and 2006  
898 seems to have stabilised between 2007 and 2010, and the fraction has even increased in 2011.  
899 The overall quantity of gas flared since 2000 has been steady between 93 and 110 bcm. An  
900 increase in total production since 2009 has brought about a corresponding increase in the  
901 quantity of gas flared. Incentives and stringent policies are not yet in place to encourage more  
902 companies and countries to partner with the World Bank in their “Zero Routine Flaring by  
903 2030” initiative.

904 Elevated concentrations of BC, CO, H<sub>2</sub>S, SO<sub>2</sub>, NO, NO<sub>2</sub> and PAH measured around flaring  
905 sites (ground based and aircraft) is indicative of the detrimental impact of gas flaring on the  
906 environment. Clusters of gas flaring sites around the tropics and near-tropic regions of the

907 world, where there is the likelihood on enhanced atmospheric mixing of the emissions into  
908 the lower and even mid-troposphere, coupled with the high temperature of the emitted plume  
909 suggests the possibility of long-range transport of these pollutants.

910 Emission factors used for BC emission from gas flaring are inadequate to estimate emission  
911 from a typical real-world gas flare as most of the fuels used in the studies for such emission  
912 factors are not representative of fuel gas from most Flow Stations around the world. In the  
913 studies that employed the mass/mole balancing technique to estimate pollutants from the  
914 combustion of hydrocarbons, estimated EFs for CO<sub>2</sub> and CO have been given, but there is no  
915 consideration of the amount of unburnt carbon given off. It should be noted that these studies  
916 did not consider flame dynamics changes in their estimations. When estimating emissions  
917 from gas flares, there is the need to ascertain the nature (regime) of the combustion flame as  
918 the flame nature and temperature plays pivotal role in determining the pollutants yield, and  
919 this has not yet been routinely considered in dispersion modelling and global inventories.

920 Global models need to update the sources of BC to include gas flaring, especially in regions  
921 prone to long-range transfer of gas flaring emission from leading gas flaring nations  
922 including Russia, Nigeria and the Middle East.

923

#### 924 **Acknowledgment**

925 Olusegun G. Fawole is highly grateful to the UK government for funding his PhD studies  
926 through the UK Commonwealth Scholarships Commission (CSCUK). The authors  
927 appreciate the anonymous reviewers for their helpful criticisms and comments.

928

929

930

931

932 **6 Glossary**

933 1. Heating value – the heat evolved per unit of a gas when it undergoes complete  
934 combustion at standard temperature and pressure. It can be measured in unit mass,  
935 unit mole or unit volume.

936 2. Higher (gross) heating value (HHV) – The heating value when all of the water present  
937 in the combustion product in gas phase condenses to liquid.

938 3. Lower (net) heating value (LHV) - The heating value when all of the water present in  
939 the combustion product remains in the gas phase.

940 4. Volumetric heating value (VHV) – Total heat evolved per unit volume of a gas.

941 5. Equivalent ratio,  $\phi$  - This is the ratio of the stoichiometric air-fuel mass ratio to the  
942 actual air-fuel mass ratio

943 6. Mtoe – Million tonnes of oil equivalent

944 7. Laminar smoke point - The length of flame from a gas jet just before the onset of the  
945 release of visible smoke.

946

947

948

949



## 950 **7 References**

- 951 Abdulkareem, A. and Odigure, J., 2006. Deterministic Model for Noise Dispersion from gas  
952 Flaring: A case study of Niger–Delta area of Nigeria. *Chemical and biochemical*  
953 *engineering quarterly*, 20(2): 157-164.
- 954 Almanza, V., Molina, L. and Sosa, G., 2012. Soot and SO<sub>2</sub> contribution to the supersites in  
955 the MILAGRO campaign from elevated flares in the Tula Refinery. *Atmospheric*  
956 *Chemistry and Physics*, 12(21): 10583-10599.
- 957 Ana, G., Sridhar, M. and Emerole, G., 2012. Polycyclic aromatic hydrocarbon burden in  
958 ambient air in selected Niger Delta communities in Nigeria. *Journal of the Air &*  
959 *Waste Management Association*, 62(1): 18-25.
- 960 Arctic Council, 2013. Recommendations to reduce black carbon and methane emissions to  
961 slow Arctic climate change, Arctic task force on short-lived climate forcers.
- 962 Avwiri, G. and Nte, F., 2004. Environmental sound quality of some selected flow stations in  
963 the Niger Delta of Nigeria. *Journal of Applied Sciences and Environmental*  
964 *Management*, 7(2): 75-77.
- 965 Barry, R.G. and Chorley, R.J., 2009. *Atmosphere, weather and climate*. Routledge.
- 966 Becker, H. and Liang, D., 1982. Total emission of soot and thermal radiation by free  
967 turbulent diffusion flames. *Combustion and Flame*, 44(1): 305-318.
- 968 Beychok, M.R., 1994. *Fundamentals of stack gas dispersion*, 63. Milton R. Beychok Irvine.
- 969 Bond, T.C., Doherty, S.J., Fahey, D., Forster, P., Berntsen, T., DeAngelo, B., Flanner, M.,  
970 Ghan, S., Kärcher, B. and Koch, D., 2013. Bounding the role of black carbon in the  
971 climate system: A scientific assessment. *Journal of Geophysical Research:*  
972 *Atmospheres*, 118(11): 5380-5552.

973 Bond, T.C., Streets, D.G., Yarber, K.F., Nelson, S.M., Woo, J.H. and Klimont, Z., 2004. A  
974 technology-based global inventory of black and organic carbon emissions from  
975 combustion. *Journal of Geophysical Research: Atmospheres* (1984–2012), 109(D14).

976 BP, 2013. *Statistical review of world energy*, British Petroleum, Great Britain  
977 [www.bp.com/statisticalreview](http://www.bp.com/statisticalreview).

978 BP, 2015. *BP Statistical Review of world energy* ([www.bp.com/statisticalreview](http://www.bp.com/statisticalreview)).

979 Burney, J. and Ramanathan, V., 2014. Recent climate and air pollution impacts on Indian  
980 agriculture. *Proceedings of the National Academy of Sciences*: 201317275.

981 CAPP, 2007. *A recommended approach to completing the national pollutant release*  
982 *inventory (NPRI) for the upstream oil and gas industry*, Canadian Association of  
983 *Petroleum Producers*, Calgary, Canada.

984 Casadio, S., Arino, O. and Serpe, D., 2012. Gas flaring monitoring from space using the  
985 ATSR instrument series. *Remote Sensing of Environment*, 116: 239-249.

986 Castineira, D. and Edgar, T.F., 2006. CFD for simulation of steam-assisted and air-assisted  
987 flare combustion systems. *Energy & fuels*, 20(3): 1044-1056.

988 Chung, S.H. and Seinfeld, J.H., 2005. Climate response of direct radiative forcing of  
989 anthropogenic black carbon. *Journal of Geophysical Research: Atmospheres* (1984–  
990 2012), 110(D11).

991 Davoudi, M., Rahimpour, M., Jokar, S., Nikbakht, F. and Abbasfard, H., 2013. The major  
992 sources of gas flaring and air contamination in the natural gas processing plants: a  
993 case study. *Journal of Natural Gas Science and Engineering*, 13: 7-19.

994 Delichatsios, M., 1993a. Smoke yields from turbulent buoyant jet flames. *Fire safety journal*,  
995 20(4): 299-311.

996 Delichatsios, M., 1993b. Transition from momentum to buoyancy-controlled turbulent jet  
997 diffusion flames and flame height relationships. *Combustion and flame*, 92(4): 349-  
998 364.

999 Delichatsios, M.A., 1987. Air entrainment into buoyant jet flames and pool fires. *Combustion  
1000 and Flame*, 70(1): 33-46.

1001 Dung, E.J., Bombom, L.S. and Agusomu, T.D., 2008. The effects of gas flaring on crops in  
1002 the Niger Delta, Nigeria. *GeoJournal*, 73(4): 297-305.

1003 E & P Forum, 1994. Methods of estimating atmospheric emission from E&P operations;  
1004 OGP Report No. 2.59/197 The Oil Industry International Exploration and Production  
1005 forum, 25-28 Old Burlington street, London. <http://www.ogp.org.uk/pubs/197.pdf>  
1006

1007 Edwards, P., Young, C., Aikin, K., deGouw, J., Dubé, W., Geiger, F., Gilman, J., Helmig, D.,  
1008 Holloway, J. and Kercher, J., 2013. Ozone photochemistry in an oil and natural gas  
1009 extraction region during winter: simulations of a snow-free season in the Uintah  
1010 Basin, Utah. *Atmospheric Chemistry and Physics*, 13(17): 8955-8971.

1011 Edwards, P.M., Brown, S.S., Roberts, J.M., Ahmadov, R., Banta, R.M., deGouw, J.A., Dube,  
1012 W.P., Field, R.A., Flynn, J.H., Gilman, J.B., Graus, M., Helmig, D., Koss, A.,  
1013 Langford, A.O., Lefer, B.L., Lerner, B.M., Li, R., Li, S.-M., McKeen, S.A., Murphy,  
1014 S.M., Parrish, D.D., Senff, C.J., Soltis, J., Stutz, J., Sweeney, C., Thompson, C.R.,  
1015 Trainer, M.K., Tsai, C., Veres, P.R., Washenfelder, R.A., Warneke, C., Wild, R.J.,  
1016 Young, C.J., Yuan, B. and Zamora, R., 2014. High winter ozone pollution from  
1017 carbonyl photolysis in an oil and gas basin. *Nature*, advance online publication.

1018 Elvidge, C.D., Baugh, K., Pack, D., Milesi, C. and Erwin, E., 2007. A twelve year record of  
1019 national and global gas flaring volumes estimated using satellite data. Boulder, CO,  
1020 NOAA National Geophysical Data Center.

1021 Elvidge, C.D., Baugh, K.E., Ziskin, D., Anderson, S. and Ghosh, T., 2011. Estimation of gas  
1022 flaring volumes using NASA MODIS fire detection products. NOAA National  
1023 Geophysical Data Center (NGDC), annual report, 8.

1024 Elvidge, C.D., Zhizhin, M., Baugh, K., Hsu, F.-C. and Ghosh, T., 2015. Methods for Global  
1025 Survey of Natural Gas Flaring from Visible Infrared Imaging Radiometer Suite Data.  
1026 *Energies*, 9(1): 14.

1027 Elvidge, C.D., Ziskin, D., Baugh, K.E., Tuttle, B.T., Ghosh, T., Pack, D.W., Erwin, E.H. and  
1028 Zhizhin, M., 2009. A fifteen year record of global natural gas flaring derived from  
1029 satellite data. *Energies*, 2(3): 595-622.

1030 Enviroware, 2012. Modelling industrial flares impacts, <http://www.enviroware.com>.

1031 European Commission, 2009. Emission Database for Global Atmospheric Research  
1032 (EDGAR), release version 4.0. <http://edgar.jrc.ec.europa.eu>, Joint Research Centre  
1033 (JRC)/Netherlands Environmental Assessment Agency (PBL), Netherlands.

1034 Feichter, J. and Stier, P., 2012. Assessment of black carbon radiative effects in climate  
1035 models. *Wiley Interdisciplinary Reviews: Climate Change*, 3(4): 359-370.

1036 Flagan, R.C. and Seinfeld, J.H., 2012. Fundamentals of air pollution engineering. Courier  
1037 Dover Publications.

1038 Flanner, M.G., Zender, C.S., Randerson, J.T. and Rasch, P.J., 2007. Present-day climate  
1039 forcing and response from black carbon in snow. *Journal of Geophysical Research:*  
1040 *Atmospheres* (1984–2012), 112(D11).

1041 Fortner, E., Brooks, W., Onasch, T., Canagaratna, M., Massoli, P., Jayne, J., Franklin, J.,  
1042 Knighton, W., Wormhoudt, J. and Worsnop, D., 2012. Particulate Emissions  
1043 Measured During the TCEQ Comprehensive Flare Emission Study. *Industrial &*  
1044 *Engineering Chemistry Research*, 51(39): 12586-12592.

1045 Gertler, A.W., Sagebiel, J.C., Dippel, W.A. and Farina, R.J., 1998. Measurements of dioxin  
1046 and furan emission factors from heavy-duty diesel vehicles. *Journal of the Air &*  
1047 *Waste Management Association*, 48(3): 276-278.

1048 GGFR, 2012. Estimated Flared Volumes from Satellite Data, 2007-2011., *Global Gas Flaring*  
1049 *Reduction*, <http://go.worldbank.org/G2OAW2DKZ0> (last accessed on January 9,  
1050 2015).

1051 GGFR, 2013. *The news flare* (issue 14), Washington DC ; World Bank.  
1052 <http://documents.worldbank.org/curated/en/2013/06/18082251/news-flare-issue-14>.

1053 Giwa, S.O., Adama, O.O. and Akinyemi, O.O., 2014. Baseline black carbon emissions for  
1054 gas flaring in the Niger Delta region of Nigeria. *Journal of Natural Gas Science and*  
1055 *Engineering*, 20: 373-379.

1056 Glassman, I., 1996. *Combustion*. Academic Press

1057 Goldberg, E.D., 1985. *Black carbon in the environment: properties and distribution*.  
1058 *Environmental science and technology (USA)*.

1059 Harris, M.M., King, G.B. and Laurendeau, N.M., 1986. Influence of temperature and  
1060 hydroxyl concentration on incipient soot formation in premixed flames. *Combustion*  
1061 *and flame*, 64(1): 99-112.

1062 Haynes, B. and Wagner, H.G., 1981. Soot formation. *Progress in Energy and Combustion*  
1063 *Science*, 7(4): 229-273.

1064 Hodgson, S., Nieuwenhuijsen, M.J., Colvile, R. and Jarup, L., 2007. Assessment of exposure  
1065 to mercury from industrial emissions: comparing “distance as a proxy” and dispersion  
1066 modelling approaches. *Occupational and environmental medicine*, 64(6): 380-388.

1067 Holden, J., 2005. *An introduction to physical geography and the environment*. Pearson  
1068 Education.

1069 Huang, K., Fu, J.S., Prikhodko, V.Y., Storey, J.M., Romanov, A., Hodson, E.L., Cresko, J.,  
1070 Morozova, I., Ignatieva, Y. and Cabaniss, J., 2015. Russian anthropogenic black  
1071 carbon: Emission reconstruction and Arctic black carbon simulation. *Journal of*  
1072 *Geophysical Research: Atmospheres*.

1073 Huang, R.F. and Wang, S.M., 1999. Characteristic flow modes of wake-stabilized jet flames  
1074 in a transverse air stream. *Combustion and Flame*, 117(1): 59-77.

1075 IEA, 2012. IEA statistics: Natural gas information, International Energy Agency.

1076 IEA, 2013. Key World Energy Statistics International Energy Agency, France.

1077 IMP, 2006. Estudio de las emisiones de la zona industrial de Tula y su impacto en la calidad  
1078 del aire regional , PS-MA-IF-F21393-1, IMP, Mexico.

1079 IPCC, 2007. Climate Change 2007: The Physical Science Basis. Contribution of Working  
1080 Group I to the Fourth Assessment Report of the Intergovernmental Panel on Climate  
1081 Change [Solomon, S., D. Qin, M. Manning, Z. Chen, M. Marquis, K.B. Averyt,  
1082 M.Tignor and H.L. Miller (eds.)]. Cambridge University Press, Cambridge, United  
1083 Kingdom and New York, NY, USA.

1084 Ismail, O.S. and Umukoro, G.E., 2014. Modelling combustion reactions for gas flaring and  
1085 its resulting emissions. *Journal of King Saud University-Engineering Sciences*:  
1086 <http://dx.doi.org/10.1016/j.jksues.2014.02.003>.

1087 Jacobson, M.Z., 2002. Control of fossil-fuel particulate black carbon and organic matter,  
1088 possibly the most effective method of slowing global warming. *Journal of*  
1089 *Geophysical Research: Atmospheres* (1984–2012), 107(D19): ACH 16-1-ACH 16-22.

1090 Johansson, J.K., Mellqvist, J., Samuelsson, J., Offerle, B., Lefer, B., Rappenglück, B., Flynn,  
1091 J. and Yarwood, G., 2014. Emission measurements of alkenes, alkanes, SO<sub>2</sub>, and  
1092 NO<sub>2</sub> from stationary sources in Southeast Texas over a 5 year period using SOF and  
1093 mobile DOAS. *Journal of Geophysical Research: Atmospheres*, 119(4): 1973-1991.

- 1094 Johnson, M., Devillers, R. and Thomson, K., 2013. A Generalized Sky-LOSA Method to  
1095 Quantify Soot/Black Carbon Emission Rates in Atmospheric Plumes of Gas Flares.  
1096 *Aerosol Science and Technology*, 47(9): 1017-1029.
- 1097 Johnson, M.R. and Coderre, A.R., 2011. An analysis of flaring and venting activity in the  
1098 Alberta upstream oil and gas industry. *Journal of the Air & Waste management*  
1099 *association*, 61(2): 190-200.
- 1100 Johnson, M.R., Devillers, R.W. and Thomson, K.A., 2011. Quantitative field measurement of  
1101 soot emission from a large gas flare using Sky-LOSA. *Environmental science &*  
1102 *technology*, 45(1): 345-350.
- 1103 Kennedy, I.M., 1997. Models of soot formation and oxidation. *Progress in Energy and*  
1104 *Combustion Science*, 23(2): 95-132.
- 1105 Klimont, Z., Smith, S.J. and Cofala, J., 2013. The last decade of global anthropogenic sulfur  
1106 dioxide: 2000–2011 emissions. *Environmental Research Letters*, 8(1): 014003.
- 1107 Koch, D., Schulz, M., Kinne, S., McNaughton, C., Spackman, J.R., Balkanski, Y., Bauer, S.,  
1108 Berntsen, T., Bond, T.C. and Boucher, O., 2009. Evaluation of black carbon  
1109 estimations in global aerosol models. *Atmospheric Chemistry and Physics*, 9(22):  
1110 9001-9026.
- 1111 Kostiuk, L., Johnson, M. and Thomas, G., 2004. University Of Alberta Flare Research  
1112 Project: final report November 1996-September 2004. 2,  
1113 [http://www.mece.ualberta.ca/groups/combustion/flare/papers/Final%20Report2004.pd](http://www.mece.ualberta.ca/groups/combustion/flare/papers/Final%20Report2004.pdf)  
1114 [f](http://www.mece.ualberta.ca/groups/combustion/flare/papers/Final%20Report2004.pdf).
- 1115 Lautenberger, C.W., de Ris, J.L., Dembsey, N.A., Barnett, J.R. and Baum, H.R., 2005. A  
1116 simplified model for soot formation and oxidation in CFD simulation of non-  
1117 premixed hydrocarbon flames. *Fire Safety Journal*, 40(2): 141-176.

1118 Law, K., Fierli, F., Cairo, F., Schlager, H., Borrmann, S., Streibel, M., Real, E., Kunkel, D.,  
1119 Schiller, C. and Ravegnani, F., 2010. “Air mass origins influencing TTL chemical  
1120 composition over West Africa during 2006 summer monsoon” published in *Atmos.*  
1121 *Chem. Phys.*, 10, 10753–10770, 2010. *Atmos. Chem. Phys.*, 10: 10939-10940.

1122 Leahey, D. and Davies, M., 1984. Observations of plume rise from sour gas flares.  
1123 *Atmospheric Environment* (1967), 18(5): 917-922.

1124 Leahey, D.M., Preston, K. and Stroscher, M., 2001. Theoretical and observational assessments  
1125 of flare efficiencies. *Journal of the Air & Waste Management Association*, 51(12):  
1126 1610-1616.

1127 Liberman, M.A., 2010. *Introduction to physics and chemistry of combustion: explosion,*  
1128 *flame, detonation.* Springer Science & Business Media.

1129 MacKay, D., 2008. *Sustainable Energy-without the hot air.* UIT Cambridge.

1130 Magnussen, B.F. and Hjertager, B.H., 1977. On mathematical modeling of turbulent  
1131 combustion with special emphasis on soot formation and combustion, *Symposium*  
1132 *(International) on Combustion.* Elsevier, pp. 719-729.

1133 Mari, C.H., Reeves, C.E., Law, K.S., Ancellet, G., Andrés-Hernández, M.D., Barret, B.,  
1134 Bechara, J., Borbon, A., Bouarar, I. and Cairo, F., 2011. Atmospheric composition of  
1135 West Africa: highlights from the AMMA international program. *Atmospheric Science*  
1136 *Letters*, 12(1): 13-18.

1137 Maricq, M.M., 2009. An examination of soot composition in premixed hydrocarbon flames  
1138 via laser ablation particle mass spectrometry. *Journal of Aerosol Science*, 40(10):  
1139 844-857.

1140 Mathon, V. and Laurent, H., 2001. Life cycle of Sahelian mesoscale convective cloud  
1141 systems. *Quarterly Journal of the Royal Meteorological Society*, 127(572): 377-406.



1142 McAllister, S., Chen, J.-Y., Fernandez-Pello, A.C., Fernandez-Pello, A.C. and Fernandez-  
1143 Pello, A.C., 2011. Fundamentals of combustion processes. Springer.

1144 McDaniel, M. and Tichenor, B.A., 1983. Flare efficiency study, US Environmental  
1145 Protection Agency, Industrial Environmental Research Laboratory,  
1146 [http://www.tceq.state.tx.us/assets/public/implementation/air/rules/Flare/Resource\\_1.p](http://www.tceq.state.tx.us/assets/public/implementation/air/rules/Flare/Resource_1.pdf)  
1147 [df](http://www.tceq.state.tx.us/assets/public/implementation/air/rules/Flare/Resource_1.pdf).

1148 McEwen, J.D. and Johnson, M.R., 2012. Black carbon particulate matter emission factors for  
1149 buoyancy-driven associated gas flares. Journal of the Air & Waste Management  
1150 Association, 62(3): 307-321.

1151 Miyauchi, T., Mori, Y. and Yamaguchi, T., 1981. Effect of steam addition on NO formation,  
1152 Symposium (International) on combustion. Elsevier, pp. 43-51.

1153 Moss, J., Stewart, C. and Syed, K., 1989. Flowfield modelling of soot formation at elevated  
1154 pressure, Symposium (International) on Combustion. Elsevier, pp. 413-423.

1155 Müller-Dethlefs, K. and Schlader, A., 1976. The effect of steam on flame temperature,  
1156 burning velocity and carbon formation in hydrocarbon flames. Combustion and flame,  
1157 27: 205-215.

1158 Nwaichi, E.O. and Uzazobona, M.A., 2011. Estimation of the CO<sub>2</sub> Level due to Gas Flaring  
1159 in the Niger Delta. Research Journal of Environmental Sciences, 5(6): 565-572.

1160 Obanijesu, E., Adebisi, F., Sonibare, J. and Okelana, O., 2009. Air-borne SO<sub>2</sub> Pollution  
1161 Monitoring in the Upstream Petroleum Operation Areas of Niger-Delta, Nigeria.  
1162 Energy Sources, Part A, 31(3): 223-231.

1163 OGP, 2000. Flaring and venting in the oil and gas exploration and production industry: An  
1164 overview of purpose, quantities, issues, practices and trends. Report No. 2.79/288,  
1165 International association of oil and gas producers UK  
1166 <http://www.ogp.org.uk/pubs/288.pdf>.

- 1167 Osuji, L.C. and Adesiyun, S.O., 2005. The Isiokpo Oil-Pipeline Leakage: Total Organic  
1168 Carbon/Organic Matter Contents of Affected Soils. *Chemistry & biodiversity*, 2(8):  
1169 1079-1085.
- 1170 Osuji, L.C. and Onojake, C.M., 2004. Trace Heavy Metals Associated with Crude Oil: A  
1171 Case Study of Ebocha-8 Oil-Spill-Polluted Site in Niger Delta, Nigeria. *Chemistry &*  
1172 *biodiversity*, 1(11): 1708-1715.
- 1173 Ouf, F.-X., Vendel, J., Coppalle, A., Weill, M. and Yon, J., 2008. Characterization of soot  
1174 particles in the plumes of over-ventilated diffusion flames. *Combustion Science and*  
1175 *Technology*, 180(4): 674-698.
- 1176 Pope III, C.A., Burnett, R.T., Thun, M.J., Calle, E.E., Krewski, D., Ito, K. and Thurston,  
1177 G.D., 2002. Lung cancer, cardiopulmonary mortality, and long-term exposure to fine  
1178 particulate air pollution. *Journal of American Medical Association*, 287(9): 1132-  
1179 1141.
- 1180 Quinn, P., Bates, T., Baum, E., Doubleday, N., Fiore, A., Flanner, M., Fridlind, A., Garrett,  
1181 T., Koch, D. and Menon, S., 2008. Short-lived pollutants in the Arctic: their climate  
1182 impact and possible mitigation strategies. *Atmospheric Chemistry and Physics*, 8(6):  
1183 1723-1735.
- 1184 Ramana, M., Ramanathan, V., Feng, Y., Yoon, S., Kim, S., Carmichael, G. and Schauer, J.,  
1185 2010. Warming influenced by the ratio of black carbon to sulphate and the black-  
1186 carbon source. *Nature Geoscience*, 3(8): 542-545.
- 1187 Ramanathan, V. and Carmichael, G., 2008. Global and regional climate changes due to black  
1188 carbon. *Nature geoscience*, 1(4): 221-227.
- 1189 Reeves, C., Formenti, P., Afif, C., Ancellet, G., Attié, J.-L., Bechara, J., Borbon, A., Cairo,  
1190 F., Coe, H. and Crumeyrolle, S., 2010. Chemical and aerosol characterisation of the

1191 troposphere over West Africa during the monsoon period as part of AMMA.  
1192 Atmospheric Chemistry and Physics, 10(16): 7575-7601.

1193 Roiger, A., Thomas, J.-L., Schlager, H., Law, K.S., Kim, J., Schäfler, A., Weinzierl, B.,  
1194 Dahlkötter, F., Krisch, I. and Marelle, L., 2015. Quantifying emerging local  
1195 anthropogenic emissions in the Arctic region: the ACCESS aircraft campaign  
1196 experiment. *bulletin of the american meteorological Society*, 96(3): 441-460.

1197 RTI, 2011. Emission protocol for petroleum refineries v 2.1.1, RTI International, Research  
1198 Triangle Park, NC 27709-2194.  
1199 [http://www.epa.gov/ttnchie1/efpac/protocol/Emission\\_Estimation\\_Protocol\\_for\\_Petroleum\\_Refinerie\\_052011.pdf](http://www.epa.gov/ttnchie1/efpac/protocol/Emission_Estimation_Protocol_for_Petroleum_Refinerie_052011.pdf).

1201 Schultz, C., 2014. Texas refinery air pollution emissions are being severely underestimated.  
1202 *Eos, Transactions American Geophysical Union*, 95(24): 208-208.

1203 Seinfeld, J., 2008. Atmospheric science: Black carbon and brown clouds. *Nature geoscience*,  
1204 1(1): 15-16.

1205 Sivathanu, Y. and Faeth, G.M., 1990. Soot volume fractions in the overfire region of  
1206 turbulent diffusion flames. *Combustion and flame*, 81(2): 133-149.

1207 Smith, D. and Chughtai, A., 1995. The surface structure and reactivity of black carbon.  
1208 *Colloids and Surfaces A: Physicochemical and Engineering Aspects*, 105(1): 47-77.

1209 Sonibare, J., Adebisi, F., Obanijesu, E. and Okelana, O., 2010. Air quality index pattern  
1210 around petroleum production facilities. *Management of Environmental Quality: An  
1211 International Journal*, 21(3): 379-392.

1212 Sonibare, J.A. and Akeredolu, F.A., 2004. A theoretical prediction of non-methane gaseous  
1213 emissions from natural gas combustion. *Energy Policy*, 32(14): 1653-1665.

1214 Stocker, T., Qin, D., Plattner, G., Tignor, M., Allen, S., Boschung, J., Nauels, A., Xia, Y.,  
1215 Bex, B. and Midgley, B., 2013. IPCC, 2013: climate change 2013: the physical

1216 science basis. Contribution of working group I to the fifth assessment report of the  
1217 intergovernmental panel on climate change.

1218 Stohl, A., Klimont, Z., Eckhardt, S., Kupiainen, K., Shevchenko, V., Kopeikin, V. and  
1219 Novigatsky, A., 2013. Black carbon in the Arctic: the underestimated role of gas  
1220 flaring and residential combustion emissions. *Atmospheric Chemistry and Physics*,  
1221 13(17): 8833-8855.

1222 Stone, D.K., Lynch, S.K., Pandullo, R.F., Evans, L.B. and Vatauvuk, W.M., 1992. Flares. Part  
1223 I: Flaring Technologies for Controlling VOC-Containing Waste Streams. *Journal of*  
1224 *the Air & Waste Management Association*, 42(3): 333-340.

1225 Strosher, M.T., 2000. Characterization of emissions from diffusion flare systems. *Journal of*  
1226 *the Air & Waste Management Association*, 50(10): 1723-1733.

1227 Sultan, B. and Janicot, S., 2003. The West African monsoon dynamics. Part II: The  
1228 “preonset” and “onset” of the summer monsoon. *Journal of climate*, 16(21): 3407-  
1229 3427.

1230 Talebi, A., Fatehifar, E., Alizadeh, R. and Kahforoushan, D., 2014. The Estimation and  
1231 Evaluation of New CO, CO<sub>2</sub>, and NO<sub>x</sub> Emission Factors for Gas Flares Using Pilot  
1232 Scale Flare. *Energy Sources, Part A: Recovery, Utilization, and Environmental*  
1233 *Effects*, 36(7): 719-726.

1234 Tesner, P., Smegiriova, T. and Knorre, V., 1971a. Kinetics of dispersed carbon formation.  
1235 *Combustion and Flame*, 17(2): 253-260.

1236 Tesner, P., Tsygankova, E., Guilazetdinov, L., Zuyev, V. and Loshakova, G., 1971b. The  
1237 formation of soot from aromatic hydrocarbons in diffusion flames of hydrocarbon-  
1238 hydrogen mixtures. *Combustion and Flame*, 17(3): 279-285.

1239 Torres, V.M., Herndon, S. and Allen, D.T., 2012a. Industrial flare performance at low flow  
1240 conditions. 2. Steam-and air-assisted flares. *Industrial & Engineering Chemistry*  
1241 *Research*, 51(39): 12569-12576.

1242 Torres, V.M., Herndon, S., Kodesh, Z. and Allen, D.T., 2012b. Industrial flare performance  
1243 at low flow conditions. 1. Study overview. *Industrial & Engineering Chemistry*  
1244 *Research*, 51(39): 12559-12568.

1245 Tripathi, S., Dey, S., Tare, V. and Satheesh, S., 2005. Aerosol black carbon radiative forcing  
1246 at an industrial city in northern India. *Geophysical Research Letters*, 32(8).

1247 Tumolva, L., Park, J.-Y., Kim, J.-s., Miller, A.L., Chow, J.C., Watson, J.G. and Park, K.,  
1248 2010. Morphological and elemental classification of freshly emitted soot particles and  
1249 atmospheric ultrafine particles using the TEM/EDS. *Aerosol Science and Technology*,  
1250 44(3): 202-215.

1251 USEPA, 1995. AP 42-Compilation of air pollutant emission factors. Section 13.5: Industrial  
1252 flares, U.S Environmental Protection Agency, Office of Air quality planning and  
1253 standards, Research Triangle Park, NC.  
1254 <http://www.epa.gov/ttn/chief/ap42/ch13/final/c13s05.pdf>.

1255 USEPA, 2000. Test Method 5-Determination of particulate matter emissions from stationary  
1256 sources, U.S Environmental Protection Agency.  
1257 [www.epa.gov/ttnemc01/methods/methods5.html](http://www.epa.gov/ttnemc01/methods/methods5.html).

1258 USEPA, 2008. Direct emissions from stationary combustion sources EPA430-K-08-003,  
1259 United States Environmental Protection Agency  
1260 <http://www.epa.gov/climateleadership/documents/resources/stationarycombustionguidance.pdf>.  
1261

1262 USEPA, 2010. Integrated Science Assessment for Particulate Matter, US Environmental  
1263 Protection Agency, Washington, DC.

1264 USEPA, 2011. Emission Estimation Protocol for Petroleum Refineries, US Environmental  
1265 Protection Agency, Washington, DC.

1266 USEPA, 2012. Report to congress on Black Carbon. EPA-450/R-12-001, United States  
1267 Environmental Protection Agency, Research Triangle Park, NC.

1268 USEPA, 2014. AP 42-Compilation of air pollutant emission factors. Section 13.5: Industrial  
1269 flares

1270 U.S Environmental Protection Agency, Office of Air quality planning and standards,  
1271 Research Triangle Park, NC.  
1272 [http://www.epa.gov/ttn/chief/ap42/ch13/final/dc13s05\\_8-19-14.pdf](http://www.epa.gov/ttn/chief/ap42/ch13/final/dc13s05_8-19-14.pdf).

1273 Villasenor, R., Magdaleno, M., Quintanar, A., Gallardo, J., López, M., Jurado, R., Miranda,  
1274 A., Aguilar, M., Melgarejo, L. and Palmerin, E., 2003. An air quality emission  
1275 inventory of offshore operations for the exploration and production of petroleum by  
1276 the Mexican oil industry. *Atmospheric Environment*, 37(26): 3713-3729.

1277 Wang, X., Heald, C., Ridley, D., Schwarz, J., Spackman, J., Perring, A., Coe, H., Liu, D. and  
1278 Clarke, A., 2014. Exploiting simultaneous observational constraints on mass and  
1279 absorption to estimate the global direct radiative forcing of black carbon and brown  
1280 carbon. *Atmospheric Chemistry and Physics*, 14(20): 10989-11010.

1281 William, F., 1985. *Combustion Theory: The fundamental theory of chemically reacting flow*  
1282 *system*. The Benjamin/Cummings Publishing Company, Menlo Park, CA.

1283 Zhang, J.J. and Morawska, L., 2002. Combustion sources of particles: 2. Emission factors  
1284 and measurement methods. *Chemosphere*, 49(9): 1059-1074.

1285

1286